OBSERVATIONS OF THE WIND AND WAVES IN HAKATA BAY

MITSUYASU, Hisashi
Research Institute for Applied Mechanics, Kyushu University : Professor

NAKAYAMA, Ryuzo
National Institute of Technology, Kitakyushu College : Recturer

KOMORI, Toshio
Research Institute for Applied Mechanics, Kyushu University : Research Associate

https://doi.org/10.5109/7172172

出版情報：Reports of Research Institute for Applied Mechanics. 19 (62), pp.37-74, 1971. 九州大学応用力学研究所
バージョン：

Reports of Research Institute for Applied Mechanics
Vol. XIX, No. 62, 1971

OBSERVATIONS OF THE WIND AND WAVES IN HAKATA BAY

By Hisashi MITSUYASU,*) Ryuzo NAKAYAMA**) and Toshio KOMORI***)

Simultaneous measurements of the wind profile over the sea surface and the wind-generated waves at short fetches have been made at an observation tower in Hakata Bay. The measurements made during the winter of 1969~1970 have revealed the following: (i) The wind profiles are described, for most cases, by the well-known logarithmic law. (ii) The wind speed above the sea surface is approximately 1.4 times greater than that above the adjacent city area. (iii) The relationships among the wind-wave-fetch parameters are consistent with wave forcasting formulas determined in our previous studies. (iv) The drag coefficient γ_{10}^2 of the sea surface increases with increasing the roughness Reynolds number $u_*\overline{H}/\nu$ introduced by Toba & Kunishi (1970), and it attains to a relatively large value, i. e., approximately to 8×10^{-3} at $u_*\overline{H}/\nu \fallingdotseq 5\times10^4$.

1. Introduction

In 1966, Hakata Bay Tower, a fixed platform for mounting the wind and wave observing equipments, was designed and constructed in Hakata Bay by 4th Regional Bureau of Port and Harbour Construction, Ministry of Transportation. Since then, efforts have been continued to measure as accurately as possible the wind and waves in the bay under various conditions.

Research Institute for Applied Mechanics of Kyushu University has had an opportunity to co-operate with that observation by developing new instruments and by analyzing various data. Some of the wind and wave data obtained during from 1967 to 1968 have been analyzed and published previously.[1),2),3)]

The present paper describes the results of the observtations made mostly during the winter of 1969~1970. As will be described later, Hakata Bay is in the north part of Kyushu island and fairly strong monsoon continues to blow

*) Professor, Research Institute for Applied Mechanics, Kyushu University.
**) Recturer, Kitakyushu Technical Colledge, Kita Kyushu.
***) Research Associate, Research Institute for Applied Mechanics, Kyushu University.

frequently in winter there. Therefore, during the period of the observation mentioned above, it has been successfully done to measure fairly strong sea winds and wind-generated waves at the bay.

One purpose of the present investigation is to make clear the wind effects on water surface. For this purpose, the wind profile over the sea surface, the wind shear stress and the water surface roughness are studied by using the wind and wave data. Another purpose is to check, under the conditions of fairly strong wind, the relationships between wind-wave parameters, i. e., the wave forcasting formulas which have been obtained in our previous papers.

2. Observing Facility and Equipments

2.1. Hakata bay

Figs. 1a and 1b show the location of Hakata Bay and the site of the observations. Hakata Bay faces to the Sea of Genkai which is a part of the Tsushima Strait. The entrance of the bay is narrowed by Genkai Shima (island), and Nokono Shima (island) divides the bay approximately into two parts, i.e., the outer part and the inner part. Owing to the effects of these two islands the wave energy coming from the outside of the bay is very small in the inner part of the bay where the observation tower has been constructed. This is an advantage for measuring the wind waves generated in the bay without being affected by the waves coming from the outside of the bay. The water depth of the inner part of the bay where the observation tower has been constructed, is relatively uniform and the depth at the tower is approximately 5 m.

2.2. The wind and waves observing tower

An observation tower in Hakata Bay has been used as a platform for mounting the wind and wave observing equipments. As shown in Fig. 2, the observation tower is a simple equilateral triangular platform which is composed essentially of three vertical piles (ϕ: 0.5 m) driven into the sea bottom. In order to minimize the disturbing effects of the platform to the wind field, the recording station has been separated from the platform and constructed on the east end of the breakwater, which is approximately 150 m south-west of the platform. Therefore, each sensor mouted on the platform has been connected to the corresponding electronic circuit and recorder through the underwater cables.

2.3. The wave gages

Capacitance-type wave gages (Denshi Kōgyō, VM-103B) have been fixed in each pile of the tower with the arm of 1.5 m length so as to reduce the effects of disturbance from the vertical main pile. The wave gages compose an equilateral triangular array of side 5 m in order to determine the directional properties of wind-generated waves. The diameter of the probe wire is ap-

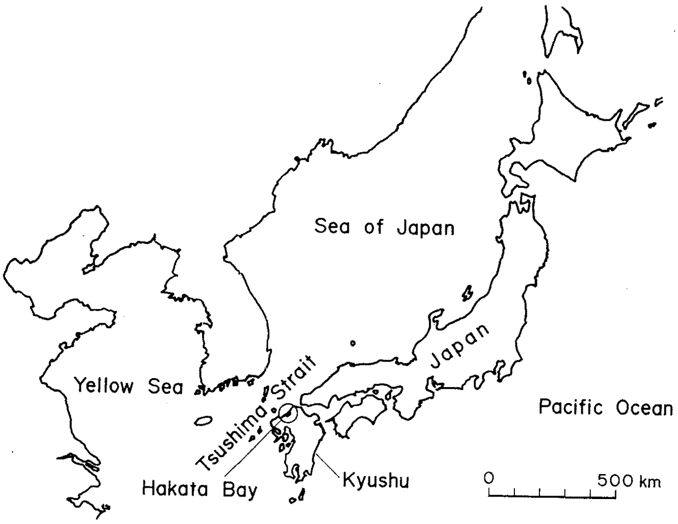

Fig. 1a Location of Hakata Bay

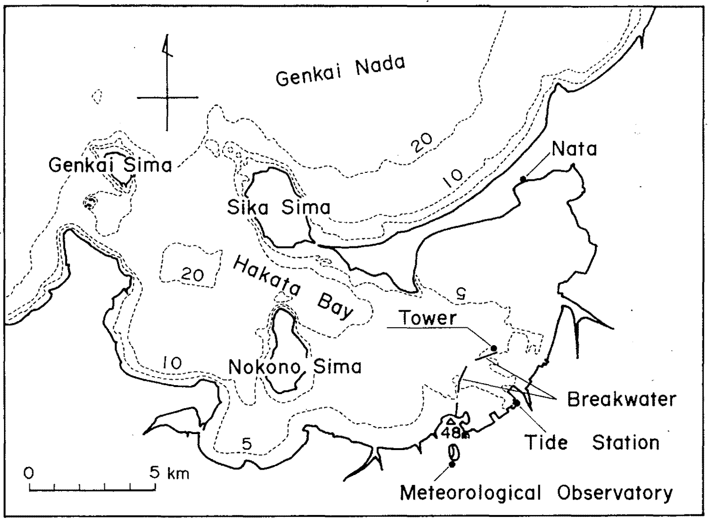

Fig. 1b Site of the observations

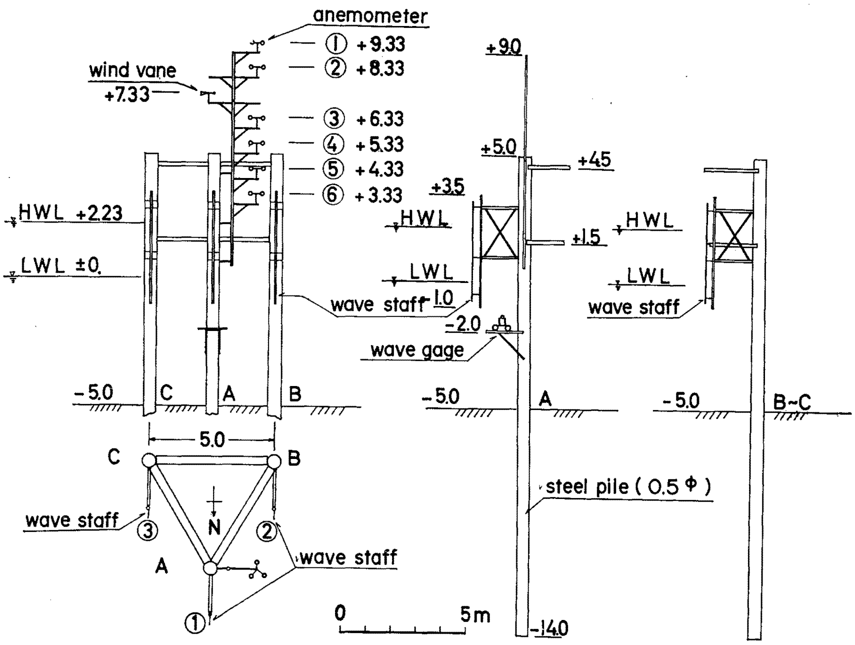

Fig. 2 Observation tower in Hakata Bay. (Unit in m)

proximately 5 mm.*) In addition to the capacitance-type wave gages, the wave gage of underwater-pressure type has been used, although the discussions in the present paper are based only on the wave data measured by one of the capacitance type wave gages.

2.4. Meteorological sensors

The wind speed and its vertical distribution were measured by six Robinson-type 3-cup anemometers in the different hights (①: 9.33 m, ②: 8.33 m, ③: 6.33 m, ④: 5.33 m, ⑤: 4.33 m, ⑥: 3.33 m, above the datum line). In usual observations, the anemometer ⑥ shown in Fig. 2 was removed, because there might be a possibility that the anemometer was broken by the hits of large waves. In the temporal observations (Rum 3) discussed later, four anemometers 3, 4,

*) Though in an original setup the insulated probe staff of 25 mm in diameter was used, this was replaced by the insulated wire of 5 mm in diameter so as to reduce the effects of surface tension.

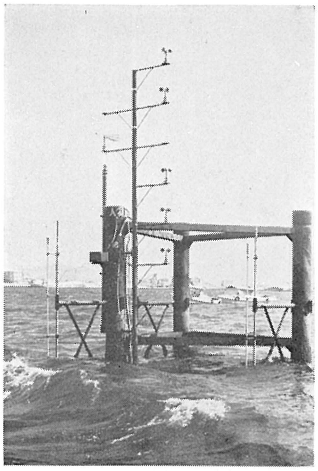

Fig. 3 Observation tower in Hakata Bay. (The photograph was taken befor the modification of the capacitance type wave gages)

(Facing p. 40)

5, and 6 were used, and the different combination of four anemometers 2, 3, 4 and 5 was used in the routine observations (Run 4, Run 5, and Run 6). Before and after a series of observations the calibrations of the anemometers were conducted in a wind tunnel of the Department of Aeronautical Engineering, Kyushu University. It was found that the calibration curves were not so different from the nominal sensitivities, within the range of the differences of $\pm 2\%$. Wind direction was measured with an wind vane which turnes a small rotational potentiometer. The special mechanical and electrical circuit was used to convert the rotation of the cup anemometer into the electric voltage. Fig. 4 schematically shows the oscillographic record of the wind speed. Each step in this record is equal to 100 m in the wind path. The measuring circuit is operated for approximately three minutes, then the potentiometer is reset to the initial position and the next measurement starts after approximately 50 sec. The average wind speed of ten minutes is determined approximately by taking the average of the wind speeds of successive three records.

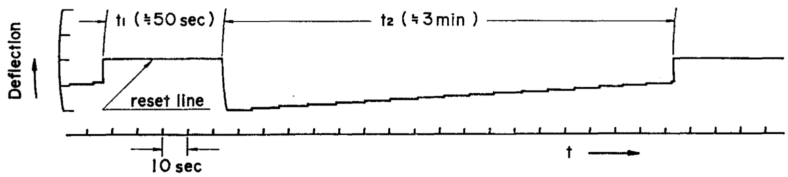

Fig. 4 Schematic diagram of the wind record

2.5. Observational procedure and controll circuit

The observations of the wind and waves reported in this paper can be tentatively classified into two types; (1) temporal (special) observation, and (2) routine (automatic) observation. Temporal or special observations can further be classified into the following cases; (i) observations served as well calibrations of the instruments, (ii) observations conducted when we went to the recording station both for checking the instruments and for exchanging the recording paper, and (iii) observations conducted for the special purposes. Several data of the observations of the case (i) were analyzed and reported previously.[1),2),3)]. A part of the previous data have been reanalyzed in the present paper (Run No. 3-1~8), because some misprints and errors in the analysis have been found in a previous paper.[2)] However, except for a few data of those temporal observations, many of the data analyzed in the present investigation have been obtained in the following routine (automatic) observation. In the routine observation, 10 minutes record has been taken at two hours interval by the underwater-pressure type wave gage. For this purpose the clock contained in the recorder of underwater-pressure type wave gage has been used. Moreover, if the wind speed at each recording period mentioned above exceeds some difinite value, which is approximately 8 m/s in the present case and can be selected arbitrary within a range of the wind speeds 0~30 m/s, the wave measurements by three gages of capacitance type, and the measurements of wind profile and wind direction have been conducted simultaneously.

For the latter purpose, a special circuit has been used, which is composed essentially of the cup anemometer with dynamo, the electronic circuit and the timer. The electronic circuit has been used for comparing the output voltage of the anemometer with the pre-set voltage corresponding to a certain value of wind speed and for switching on the electricity supply for the measuring circuits of the wind profile, the wave recorder of capacitance type and the ink wrighting oscillograph. The timer has been used for switching off the electricity supply after a certain decided time (10 minutes in the present case) from the time of switching on. In the present cases of observations, the clock and the controll circuit mentioned above have been connected in series, and the total controll circuit can be considered as "and" circuit. Therefore, the measurements of the waves by the capacitance type wave gages and the measurements of the wind profile and wind direction have been made only when the wind speed exceeds approximately 8 m/s during the measuring period of 10 minutes at two hours intervals. Although the measurement can be continued 10 minutes by the timer even when the wind speed dropped down below the pre-set value, the measurements stopped if the clock circuit turn to "off". Therefore, the measuring time is shorter than 10 minutes for such special cases that the wind speed reaches to the pre-set value slightly after the clock circuit has turned to "on". For this reason some of the data have been shorter than 10 minutes. Total instrumentations are shown schematically in Fig. 5. The remote controll switch in the figure was not used in the present observations.

3. Meteorological Conditions

3.1. Synoptic situation and meteorological elements

The data used in the present investigation were obtained in late autumn through winter. Except for some special cases in which the winds were caused by the typhoon passing off the Pacific coast of Japan, most of the winds were typical monsoon in winter season of Japan. The weather charts during the observations have been compiled in Appendix of the paper. Some meteorological elements during the observations have been listed in the right side columns of Table 2 which will be discussed later. Those data have been measured in Fukuoka Meteorological Observatory, which is approximately 4.5 km to the south-west of the platform.

3.2. Temperatures

Unfortunately, during the routine observations reported in the present paper, temperature sensors were not equipped to the tower. Therefore, the simultaneous measurements of the temperatures of the air and water near the observation tower could not been done in the present observations of the wind and

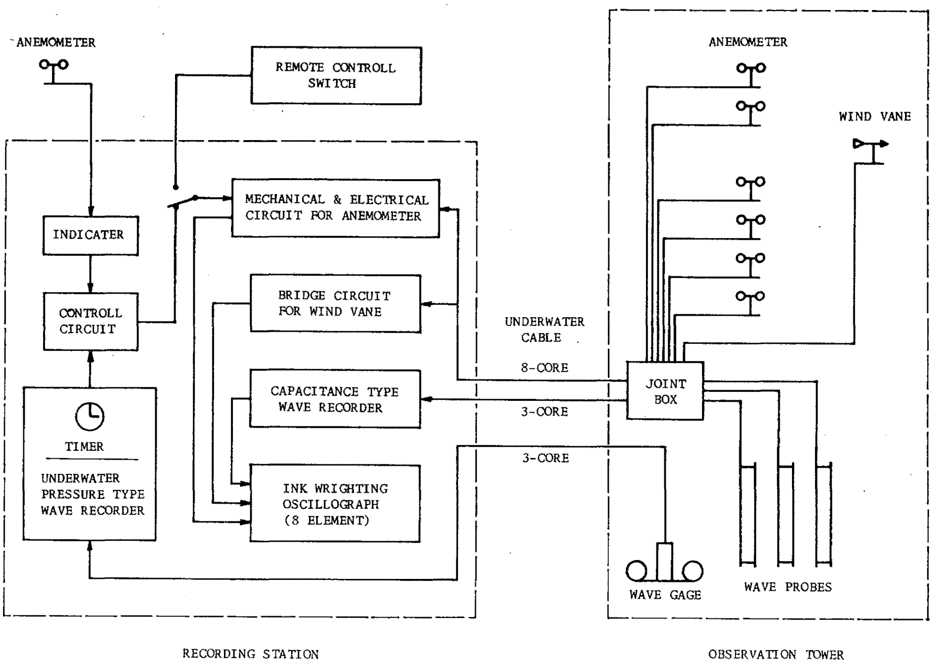

Fig. 5 Block diagram of the measuring system

waves except for the temporal observations which were made only when we went to the recording station. Therefore, as the reference materials for the air and water temperatures, the following data have been compiled in Table 2; the water temperature measured in Nata fishing port at 10 am, and the air temperature measured in Fukuoka Meteorological Observatory at the corresponding time of our wind and waves observations (as for locations see Fig. 1b).

In the temporal observations, air temparatures were measured by the dry bulb of the Assman-type psychrometer (Shimazu Co, 6-88) at about 1 m above the sea surface. The surface temperature of sea water at near the recording station was also measured by mercury thermometer. Table 1. shows the comparison of the air temperatures measured at Fukuoka Meteorological Observatory and those at the tower, and also the comparison of the water temperatures measured at Nata fishing port and those at the tower. From the results shown in Table 1, it can be seen that the differences of the air temperatures are fairly small when the weather is cloudy but the air temperature in Fukuoka Meteorological Observatory is approximately 3°C higher than that in the tower when the weather is fine. Table 1 also shows that the water temperatures measured in the tower are 0.7°C～2.5°C higher than those in the Nata fishing port.

Table 1 The temperatures of the air and water at the tower compared respectively with the air temperature at Fukuoka Meteorological Observatory and with the water temparature at Nata fishing port

Date	Time	Air temperalure (°C)		Water temperature (°C)		U_{10}(m/s)	Weather
		FMO	Tower	Nata	Tower	Tower	
9/21/'66	10:00	24.4	21.5	21.0	—	2.7	fine
	10:20	24.7	22.0	—	23.0	3.6	
	11:31	25.6	22.7	—	23.5	5.2	
	12:05	25.8	22.5	—	23.5	7.3	
	13:22	25.0	22.6	—	23.5	7.7	
	14:07	26.2	22.8	—	23.5	8.2	
10/4/'66	10:00	21.9	—	21.0	—	—	claudy
	12:20	23.0	22.0	—	22.4	2.7	
10/22/'68	10:00	18.0	—	17.5	—	—	fine
	11:02	21.2	19.2	—	19.8	4.3	
	11:28	21.8	19.3	—	19.8	5.5	
	11:49	22.8	19.6	—	19.8	6.2	
	12:22	22.2	19.3	—	19.9	7.4	
	12:53	21.7	18.7	—	20.0	7.5	
	13:19	21.7	18.3	—	20.0	7.8	
	13:35	21.7	18.6	—	20.0	9.1	
	13:48	21.8	18.6	—	20.0	9.4	
11/18/'69	10:00	9.5	—	13.0	—	—	claudy
	10:23	9.5	10.8	—	13.7	7.6	

3.3. Change of the wind speed

As was described in the previous section **2.5** the routine observations, i. e., automatic recording of the wind and waves at the tower were made only when the wind speed exceeded aprroximately to 8 m/s during the observation time of 10 min at the intervals of two hours. Consequently, the wind data are fragmentary. In order to check the duration of the wind or to see how the wind speed has changed before and after the observation time, the change of the wind at Fukuoka Meteorological Observatory are shown in Figs. 6.1 through 6.3. In these figures the wind speed U_{10} at the tower has been shown too. From the results shown in Figs. 6.1 through 6.3 it can be seen that the durations of the winds have been fairly long in most of the cases.

The minimum duration t_m, which is a length of time it takes a given wind blowing over a definite fetch length to cause a steady state condition of the wave, has been estimated as 45 min~60 min in most of the cases. Therefore, the wind waves generated in the bay can be considered approximately as fully developed waves with respect to time except for a few case of Run 3.

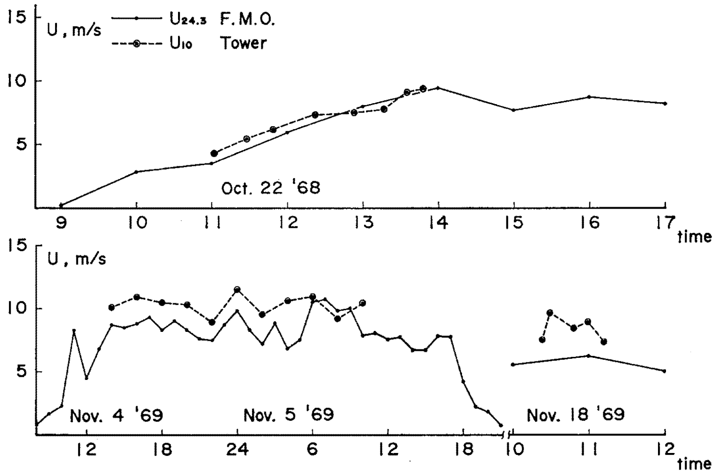

Fig. 6.1 Change of the wind speed during the observations

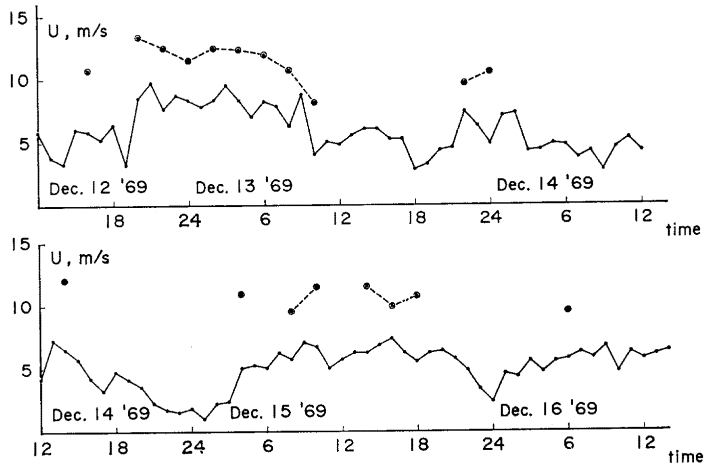

Fig. 6.2 Change of the wind speed during the observations

4. Results and Discussions

4.1. Wind profiles over sea waves

The mean speed U of approximately 10 min were plotted against the logarithm of the height z. The heights of anemometers above the sea surface in each measuring time were determined by correcting the effects of the height of the tide η simultaneously measured at the tide station in Hakata Bay (Fig. 1b), and of the subsidence of the tower (approximately 17 cm).*) Wind profiles

*) The elevations of the various parts of the tower shown in Fig. 2 were measured when the tower was constructed. However, it was found, in September 1969, that the tower had subsided approximately 17 cm.

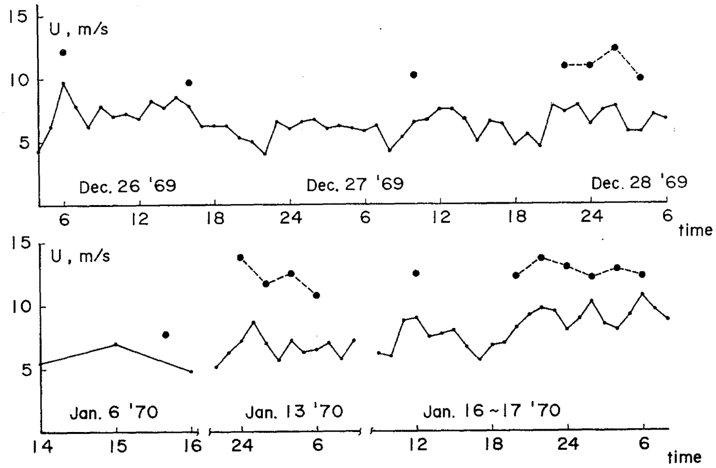

Fig. 6.3 Change of the wind speed during the observations

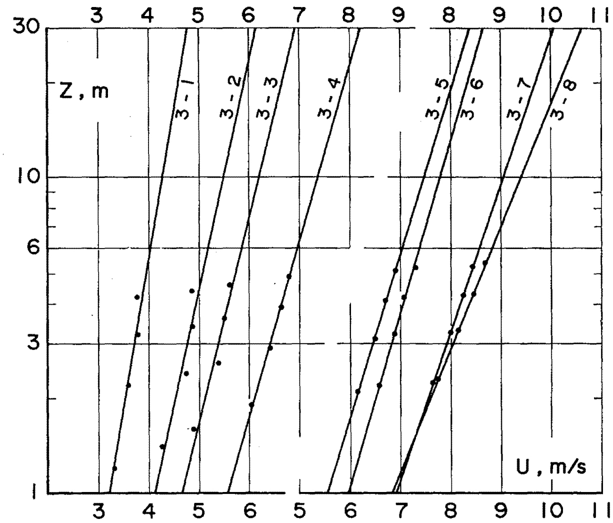

Fig. 7.1 Wind profiles over sea surface

obtained are summarized in Figs. 7.1 through 7.5. As shown in these figures, within the range of the height $z \doteqdot 2\,\mathrm{m} \sim 7\,\mathrm{m}$, the wind profiles over sea surface are described approximately by the well-known logarithmic law;

$$U = \frac{u_*}{K} ln \frac{z}{z_0}, \tag{1}$$

where U is the wind speed at the height of z, K von Kármán's constant ($\doteqdot$ 0.4), and z_0 the roughness parameter. u_* is the friction velocity defined by

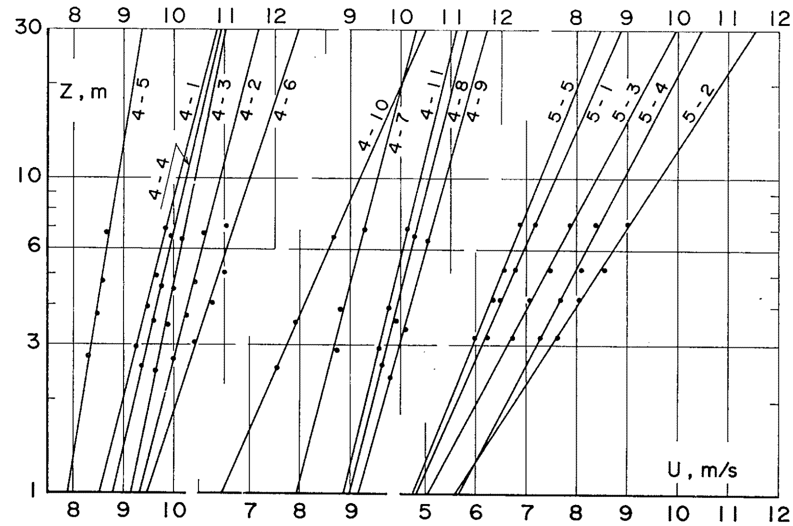

Fig. 7.2 Wind profiles over sea surface

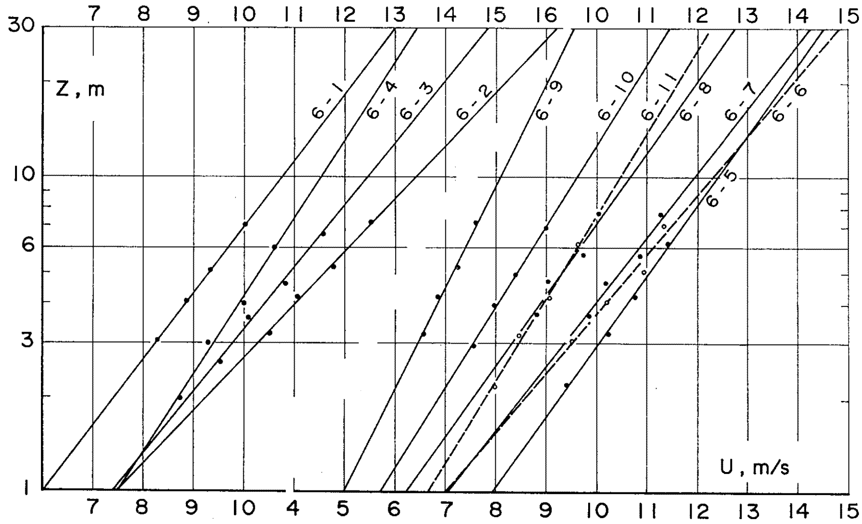

Fig. 7.3 Wind profiles over sea surface

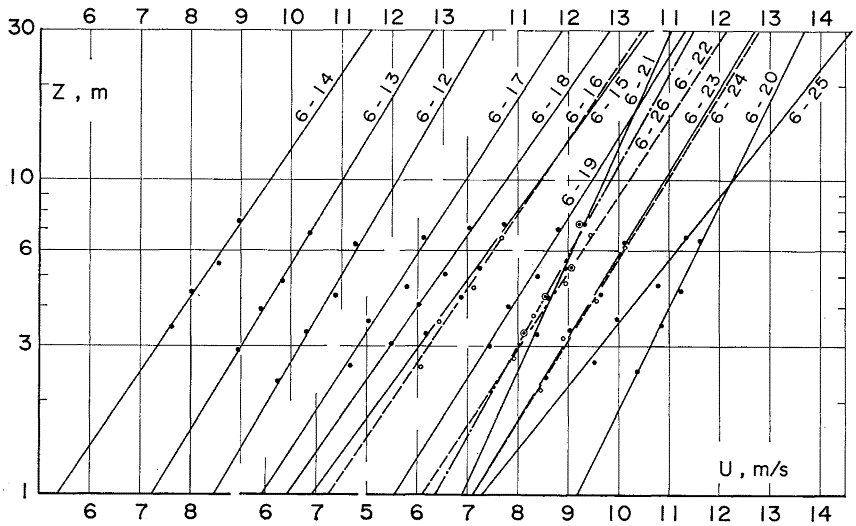

Fig. 7.4 Wind profiles over sea surface

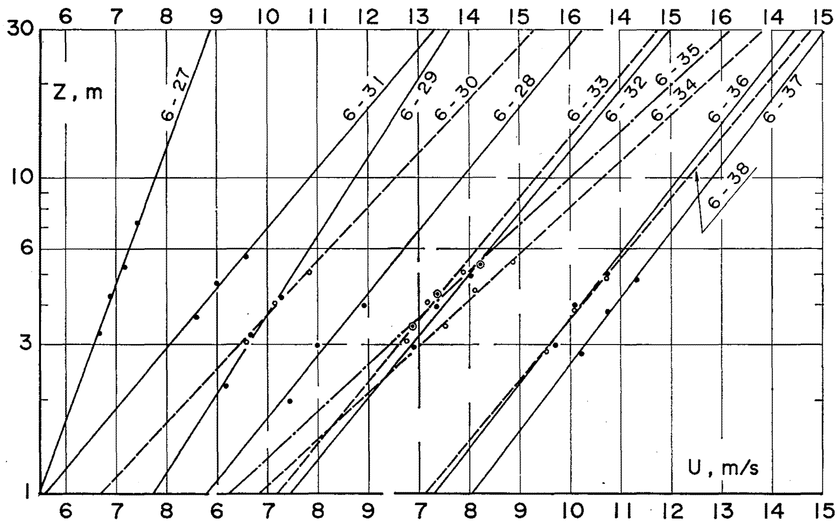

Fig. 7.5 Wind profiles over sea surface

$$u_* = \sqrt{\frac{\tau_0}{\rho}}, \tag{2}$$

where τ_0 is the shear stress of the wind exerted on the sea surface and ρ the density of the air.

Observed values of U and z were used for determining, by the method of least squares, the values of u_* and z_0 in Eq. (1). Further, since the following equation can be derived from Eq. (1)

$$U_{10}=\frac{u_*}{K}ln\frac{10^3}{z_0}, \tag{3}$$

U_{10}, the wind velocity at $z=10$ m can be detemined from the value of u_*, K and z_0 (cm). The determined values of u_*, z_0 and U_{10} are summarized in Tables. 2.1. through 2.4.

The discussions should be done here on the effects of thermal stratification of the air, since the logarithmic profile of the wind velocity is satisfied, in a strict sence, only for neutral air. As was discussed in 3.1, the temperatures of the air and that of the water were not measured at the tower in most of the present observations. Therefore, the detailed analysis of the data is difficult at this time. However, referring the water temperatures measured in Nata fishing port and the air temperatures measured in Fukuoka Meteorological Observatory which have been shown in Tables 2.2 through 2.4 and recalling the data shown in Table 1 and the discussions done in 3.1, the air is considered to have been fairly unstable in many of the cases of our wind and wave observations. In facts, closer examinations of the wind profiles shown in Figs. 7.1 through 7.5, show that the wind profiles, for examples, of Run 4-6, Run 5-4, Run 6-2, and Run 6-12 systematically deviate from the logarithmic distributions and are concave upward, which is characteristic of the wind profile of the unstable air.[4] However, many of the measured wind profiles fit well to Eq. (1), though the air is considered to have been unstable even in many of those cases. Explanations for this result will be given as follows:

In the case of near-neutral conditions of the air, the wind profiles are approximately given by the following "log+linear" profiles

$$U=\frac{u_*}{K}\left(ln\frac{z}{z_0}+\beta\frac{z}{L}\right), \tag{4}$$

where β is a constant of the order 0.6~6 and to be determined empirically. L is called "stability length" and defined by

$$L=-\frac{\rho C_p T_0 u_*^3}{gKH}, \tag{5}$$

where C_p is specific heat at constant pressure, T_0 mean absolute air temperature of the bottom layer, g the acceleration of gravity, and H the vertical heat flux. L can be defind also in a gradient form[7] as

$$L=\frac{K_m T_0 u_* (\partial U/\partial z)}{K_h gK(\partial\theta/\partial z)}, \tag{6}$$

where θ is the potetial temperature and K_m and K_h are the eddy viscosity and the eddy conductivity defined respectively by

$$u_*^2=K_m\frac{\partial U}{\partial z}, \tag{7}$$

Table 2.1 Wind data and meteorological and oceanographical conditions

Run No.	Date	Time	Hakata Bay Tower							Fukuoka Meteorological Observatory			
			D	$\bar{U}_{10}$	u_*	z_0	η	T_w	T_a	D	$U_{24.3}$	P	T_a'
				m/s	m/s	cm	m	°C	°C		m/s	mb	°C
3 — 1	10/22/'68	11 : 02	28°	4.3	0.19	9.5×10^{-2}	2.08	19.8	19.2	2	3.6	1019.5	21.2
3 — 2	〃	11 : 28	2°	5.5	0.24	1.1×10^{-1}	1.90	19.8	19.3	2	4.7	1019.1	22.2
3 — 3	〃	11 : 49	1°	6.2	0.27	1.0×10^{-1}	1.72	19.8	19.6	1	5.5	1018.7	22.6
3 — 4	〃	12 : 22	-23°	7.4	0.32	8.8×10^{-2}	1.43	19.9	19.3	16	6.7	1018.1	22.3
3 — 5	〃	12 : 53	-27°	7.5	0.34	1.4×10^{-1}	1.21	20.0	18.7	16	7.8	1017.6	21.6
3 — 6	〃	13 : 19	-25°	7.8	0.31	4.8×10^{-2}	1.10	20.0	18.3	16	8.5	1017.3	21.6
3 — 7	〃	13 : 35	-20°	9.1	0.38	6.8×10^{-2}	1.03	20.0	18.6	16	8.9	1017.1	21.7
3 — 8	〃	13 : 48	-21°	9.4	0.46	2.6×10^{-1}	0.97	20.0	18.6	16	10.2	1016.9	21.8

D: wind direction, η: tidal height above the datum line, T_w: surface temperature of the water, T_a: temperature of the air at about 1 m above the sea surface near the tower, P: atmospheric pressure, T'_a: temperature of the air at Fukuoka Meteorological Observatory.

Table 2.2 Wind data and meteorological and oceanographical conditions

Run No.	Date	Time	Hakata Bay Tower					Nata	Fukuoka Meteorological Observatory				
			D	U_{10}	u_*	z_0	η	T_w'	D	$U_{24.3}$	P	T_a'	weather*)
				m/s	m/s	m	m	°C		m/s	mb	°C	
4 — 1	11/4/'69	14 : 00	—12°	10.1	0.28	4.2×10^{-6}	1.20	17.0	16	8.7	1020.9	16.7	⌽
4 — 2	〃	16 : 00	— 9°	10.9	0.28	1.3×10^{-6}	1.47		16	8.8	1021.0	14.8	
4 — 3	〃	18 : 00	— 5°	10.4	0.22	6.1×10^{-8}	1.69		16	8.3	1021.3	13.1	⌽
4 — 4	〃	20 : 00	—15°	10.2	0.25	8.0×10^{-7}	1.63		16	8.3	1021.8	12.9	⌽
4 — 5	〃	22 : 00	+ 3°	8.9	0.17	9.2×10^{-9}	1.40		16	7.5	1021.9	12.7	
4 — 6	11/5/'69	00 : 00	—27°	11.5	0.35	2.2×10^{-5}	1.15		16	9.8	1021.6	12.5	⌽
4 — 7	〃	2 : 00	—26°	9.6	0.28	1.1×10^{-5}	1.28		16	7.2	1021.5	12.0	◎
4 — 8	〃	4 : 00	—16°	10.6	0.27	1.6×10^{-6}	1.59		16	6.8	1020.9	12.4	
4 — 9	〃	6 : 00	—19°	10.9	0.30	4.8×10^{-6}	1.81		16	10.5	1020.8	12.5	◎
4 —10	〃	8 : 00	—41°	9.2	0.48	4.8×10^{-3}	1.64		16	9.8	1021.8	12.7	●▽
4 —11	〃	10 : 00	—20°	10.4	0.26	1.4×10^{-6}	1.25	15.0	16	7.7	1022.0	13.3	
5 — 1	11/18/'69	10 : 23	—70°	7.6	0.48	1.8×10^{-2}	0.99	13.0	12	5.1	1023.5	9.5	◎
5 — 2	〃	10 : 29	—64°	9.6	0.71	4.3 〃	0.99		12	4.9	1023.4	9.5	
5 — 3	〃	10 : 48	—75°	8.4	0.58	3.1 〃	1.00		13	5.0	1023.4	9.5	
5 — 4	〃	10 : 59	—82°	8.9	0.57	1.8 〃	1.01		13	6.2	1023.3	9.5	◎
5 — 5	〃	11 : 12	—88°	7.3	0.44	1.3 〃	1.00		13	4.8	1023.3	9.5	

T_w' : water temperature measured every 10 am at Nata fishing port.

*) Weather Symbols ; ○ : very fine, ⌽ : fine, ◎ : claudy,

(Japanese style) ⊛ : snow, ●▽ : occasional light rain,

*▽ : occasional light snow.

Table 2.3 Wind data and meteorological and oceanographical conditions

Run No.	Date	Time	Hakata Bay Tower					Nata	Fukuoka Meteorological Observatory				
			D	U_{10}	u_*	z_0	η	T_w'	D	$U_{24.6}$	P	T_a'	wether
				m/s	m/s	m	m	°C		m/s	mb	°C	
6 — 1	12/12/'69	16 : 00	—57°	10.7	0.82	5.4×10^{-2}	1.13	8.5	12	5.8	1015.2	10.0	◎
6 — 2	〃	20 : 00	—66°	13.4	1.02	5.3 〃	0.97		12	8.5	1017.3	8.1	
6 — 3	〃	22 : 00	—40°	12.5	0.88	3.4 〃	1.57		13	7.7	1017.8	6.9	⦶
6 — 4	12/13/'69	00 : 00	—57°	11.5	0.71	1.4 〃	2.19		13	8.3	1017.8	6.1	⦶
6 — 5	〃	2 : 00	—56°	12.4	0.78	1.7 〃	1.96		13	8.3	1018.2	5.2	
6 — 6	〃	4 : 00	—56°	12.3	0.93	4.9 〃	1.12		13	8.3	1019.0	3.9	◎
6 — 7	〃	6 : 00	—82°	11.9	0.84	3.5 〃	0.50		13	8.2	0119.1	3.2	◎
6 — 8	〃	8 : 00	—63°	10.6	0.77	3.9 〃	0.46		12	6.2	1019.8	2.9	$\overset{*}{\triangledown}$
6 — 9	〃	10 : 00	—55°	8.1	0.54	2.5 〃	0.96	6.0	14	4.0	1021.0	0.9	
6 —10	〃	22 : 00	—72°	9.6	0.67	3.3 〃	1.23		12	7.3	1019.9	3.8	$\overset{*}{\triangledown}$
6 —11	12/14/'69	00 : 00	—57°	10.5	0.65	1.7 〃	2.00		12	4.8	1020.0	4.2	◎
6 —12	〃	14 : 00	—84°	12.1	0.63	4.7×10^{-3}	1.86	7.0	13	6.5	1021.0	4.9	
6 —13	12/15/'69	4 : 00	—55°	11.0	0.65	1.2×10^{-2}	1.36		13	5.0	1021.7	6.3	◎
6 —14	〃	8 : 00	—80°	9.6	0.73	5.3 〃	0.74		13	5.7	1022.3	6.9	◎
6 —15	〃	10 : 00	—81°	11.4	0.78	2.8 〃	0.89	6.0	13	6.7	1022.4	7.7	◎
6 —16	〃	14 : 00	—73°	11.5	0.73	1.8 〃	1.59		14	6.2	1021.2	8.2	◎
6 —17	〃	16 : 00	—68°	10.0	0.70	3.3 〃	1.57		13	7.3	1022.2	8.1	◎
6 —18	〃	18 : 00	—83°	10.8	0.75	3.3 〃	1.13		13	5.5	1023.2	7.0	⦶
6 —19	12/16/'69	6 : 00	—70°	9.5	0.68	3.8 〃	1.18	6.0	13	5.7	1024.0	6.0	⦶

Table 2.4 Wind data and meteorological and oceanographical conditions

Run No.	Date	Time	Hakata Bay Tower					Nata	Fukuoka Meteorological Observatory				
			D	U_{10}	u_*	z_0	η	T_w'	D	$U_{24.3}$	P	T_a'	weather
				m/s	m/s	m	m	°C		m/s	mb	°C	
6—20	12/26/'69	6:00	−14°	12.2	0.53	9.2×10^{-4}	1.67	8.0	16	9.7	1014.3	10.8	●▽
6—21	〃	16:00	−26°	9.7	0.49	3.4×10^{-3}	0.91		16	7.8	1019.2	8.7	⦶
6—22	12/27/'69	10:00	−72°	10.2	0.71	3.3×10^{-2}	1.44	7.0	13	6.5	1026.0	2.7	◎
6—23	〃	22:00	−79°	10.9	0.66	1.3 〃	1.80		12	7.3	1025.2	2.3	◎
6—24	12/28/'69	00:00	−66°	10.9	0.67	1.4 〃	1.99		12	6.3	1025.0	1.9	⦶
6—25	〃	2:00	−76°	12.3	0.85	3.2 〃	1.49	6.0	13	7.7	1025.2	2.2	◎
6—26	〃	4:00	−60°	9.8	0.60	1.5 〃	0.86		13	5.7	1025.8	2.7	
6—27	1/6/'70	15:40	−127°	7.8	0.40	4.1×10^{-3}	0.92	6.0					◎
6—28	1/13/'70	00:00	−80°	13.9	0.88	1.8×10^{-2}	2.18	6.0	12	7.2	1018.0	11.1	⊛
6—29	〃	2:00	−78°	11.7	0.69	1.1 〃	1.96	6.0	13	7.0	1020.0	9.3	○
6—30	〃	4:00	−68°	12.5	1.01	6.8 〃	1.12		13	7.2	1021.0	8.0	
6—31	〃	6:00	−73°	10.8	0.92	8.8 〃	0.50		12	6.5	1021.7	6.6	○
6—32	1/16/'70	12:00	−85°	12.5	0.88	3.4 〃	1.23	4.5	13	9.0	1021.9	1.9	◎
6—33	〃	20:00	−94°	12.3	0.89	3.8 〃	1.10		12	8.2	1022.6	0.9	◎
6—34	〃	22:00	−86°	13.6	1.19	1.0×10^{-1}	0.74		13	9.7	1022.8	1.3	
6—35	1/17/'70	00:00	−70°	13.0	1.17	1.2 〃	0.82		13	8.0	1022.7	1.1	◎
6—36	〃	2:00	−69°	12.1	0.84	3.0×10^{-2}	1.17	4.5	13	10.2	1022.3	1.0	⦶
6—37	〃	4:00	−67°	12.8	0.82	1.9 〃	1.36		14	8.0	1022.5	0.7	
6—38	〃	6:00	−66°	12.3	0.90	4.1 〃	1.31		15	10.7	1023.5	0.3	⦶

and

$$H=-K_h\rho C_p\frac{\partial\theta}{\partial z}. \tag{8}$$

Quite rough estimation of the values of L by Eq. (6), showed that the order of the magnitude of L meight be 10^4 cm.*) If this is true, the second term $\beta z/L$ in the right side bracket of Eq. (4) is approximately 0.2, where β has been assumed tentatively to be 4 and z has been taken as 5×10^2 cm. Since the order of the magnitude of $ln\ z/z_0$ is $2\sim5$, the second term is much smaller than the first term. Therefore, the effects of thermal stratifications would be very small for the wind profiles at nearby $z=5$ m.

Several investigators reported the existence of a kink in the wind profile near the water surface.[8),9)] However, as shown in Figs. 7.1 through 7.5, the kinks in the wind profiles are not so clear in our present observations, except for the tendencies that the wind speeds measured by the second anemometer from the top are relatively large and those measured by the third anemometer from the top are relatively small in some of the wind profiles. Although such tendencies are remarkable in the wind profiles, for examples, of Run 6–7, 6–8, 6–17 and 6–25, their explanations are difficult at present now. Since each anemometer was calibrated just after the present observations, i.e., (in January 28, 1970), and the change of the sensitivity of each anemometer was never found, the above facts could not be attributed to the instrumental errors. Moreover, as shown in Fig. 2, anemometers were mounted on the north side of the tower and the wind directions during the observations were $N\sim NW$. Thus, the effects of the tower on the measured wind profiles would be neglisible. The likeliest explanation is the shortness of the averaging time of the wind velocity. In fact, it was found that many of the wind profiles showed zigzag form when their averaging time was not long, and they became gradually smooth profiles as increasing the averaging time.

Finally, some remarks are made on the effect of wind-wave interacions. As will be shown later, in many cases, the wave period during the wind observations was in the range $T_{1/3}=2$ sec$\sim$3 sec, and thus the phase velocity C of the wave would be approximately $C=3$m/s$\sim$5m/s. As can be seen from the wind profiles shown in Figs. 7.1. through 7.5, the critical height z_c at which $U=C$, is much below the lowest level of our wind observations.

Therefore, the effect of the wind-wave interaction on the wind profiles,

---

*) *Eq.* (6) can be simplified approximately as

$$L=\frac{K_mT_0u_*(U_a-U_w)}{K_hgK(\theta_a-\theta_w)}, \tag{i}$$

where U_a is the wind velocity at some reference height, U_w the surface velocity of the water, θ_a the air temperature at some reference height, and θ_w the surfce water temperature. Assuming $K_m/K_h=1$, $u_*=50$ cm/s, $U_a=10^3$ cm/s, $U_w=0$, $g=980$ dyn/s, $K=0.4$, $\theta_a-\theta_w=3$, it becomes, from *Eq.* (i)

$L=1.2\times10^4$ cm.

which has been pointed out by Stewart (1961)[10] will not be expected in the present observations.

4.2. The relationship between the wind over the sea and that over the adjacent land

In many cases, a few or no data is available for the wind directly measured over the sea surface. Therefore, it is often necessary, for such practical purpose as wave forcasting, to estimate the wind field over the sea surface from that measured over the adjacent land surface. In order to obtain the relationship between the wind speed over the water surface in Hakata Bay and that measured in Fukuoka Meteorological Observatory (F. M. O.), the wind speed measured in Hakata Bay tower was compared, with that measured, at the same time, in F. M. O.. It was impossible to compare those wind speeds at the same elevations, because the height of the anemometer in F. M. O. was 24.3 m but the height of our highest anemometer used in the present observations was 8.16 m (=8.33 m–0.17 m). Therefore, in Fig. 8 the wind speed $U_{24.3}$ at F. M. O. has been compared with the wind U_{10} at the tower which has been obtained from the measured wind profile over the sea surface by using Eq. (3). One of the reasons for the selection of U_{10} is that U_{10} is used, in many cases, for the relationships of wind-wave parameters, and that the essential feature of the

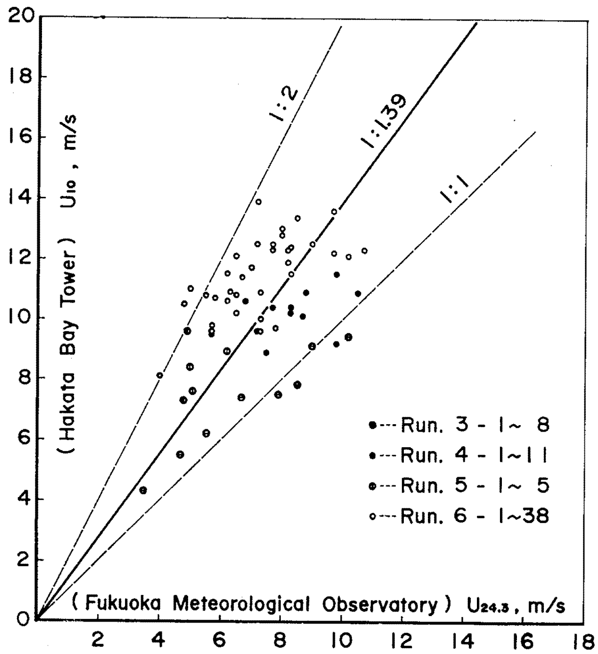

Fig. 8 Comparison of the wind speed over the sea and that over the adjacent city area. (The same symbols will be used hereafter in the figures)

relationship shown in Fig. 8 does not change very much even when $U_{8.16}$*) is selected as the wind speed at the tower. From Fig. 8, it is clear that the wind speed U_{10} measured at Hakata Bay Tower is much faster than the wind speed $U_{24.3}$ measured at F. M. O.. The ratio of U_{10} at the tower to $U_{24.3}$ at F. M. O. is 1.39: 1 in the mean, though the data are scattered between 1: 1 and 2: 1. The ratio 1.39: 1 is comparable but slightly larger than the ratio 100: 79 which has been obtained by Hunt (1956)[11] at Lake Okeechobee for the wind blowing from the lake to the land. Closer examination of Fig. 8, however, reveals that the ratio is slightly different for the different Run. For example, the ratio for Run 3 is very close to 1: 1, but the data of Run 4 are scattered between 1: 1 and 1.39: 1, and those of Run 5 and 6 are scattered between 1.39: 1 and 2: 1. When we consider that the wind of Run 3 has been an ordinary sea wind of a fine day in autumn, the wind of Run 4 has been caused by Typhoon passed off the Pacific coast of Japan, and the winds of Run 5 and Run 6 have been due to monsoon the above differences seem to be due to the differences in the meteorological conditions, though the mechanism causing such differences is not clear.

Fig. 9 shows the relation between the wind direction measured at the

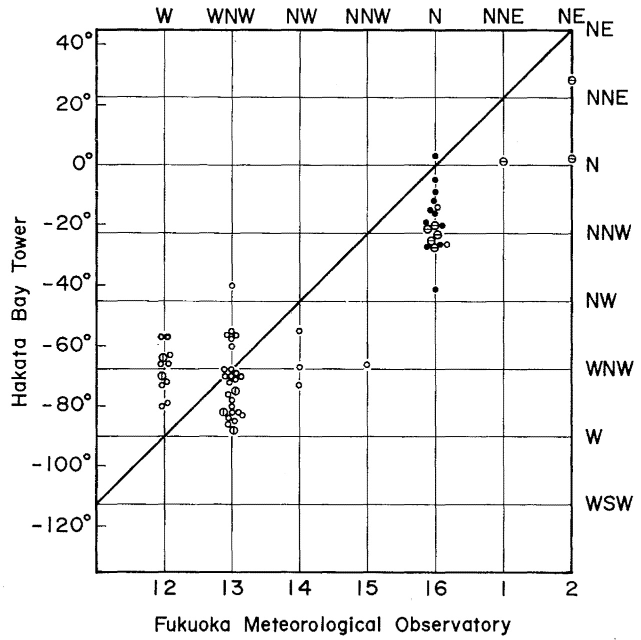

Fig. 9 Comparison of the wind direction over the sea and that over the adjacent city area.

*) $U_{8.16}$ is the wind speed measured by the highest anemometer used in the routine observations. The height of the anemometer is 8.16 m (=8.33−0.17 m).

tower and that measured at F. M. O.. From Fig. 9 it can be seen that the wind directions at the tower are roughly equal to those of F. M. O., that the directions of the fairly strong winds at the tower are concentrated around two directions NNW and WNW, and that the wind of the direction NNW at the tower has a trend to shift to the direction N at F. M. O..*)

Finally, some remarks are done on the site of Fukuoka Meteorological Observatory. Fukuoka Meteorological Observatory is in a sity area around which there are quite a few tall buildings except for private houses of one-story house or two-story house. A small hill of approximately 48 m high is about 1.7 km north of F. M. O.. Therefore, some effects of the hill on the north wind will be expected and that may explain small differences in the directions of north winds measured respctively at the tower and at F. M. O.. The small pond in the north side of F. M. O. will not so affect the wind measured at the height $z=$ 24.3. m. The distances from F. M. O. to the shore line are approximately 2.5 km to the N-direction and 1.7 km to the WNW-direction which is one of the directions of the dominant wind in winter season.

The surface roughness of the city area is much larger than that of the sea surface. Therefore, the difference in the wind speed between the tower and F. M. O. should be analyzed basically by using the results of recent studies[12),13)] on wind and shear stress profiles above a change in surface roughness. The investigation of this possibility must be the subject of future research.

4.3. Wind waves at short fetches

All wave data obtained in the present investigation are summarized in Tables 3.1 through 3.4. In each table, the measured values of the following quanties are shown: F the fetch distance, F_e the effective fetch determined by the same procedure with that presented in "Shore Protection Planning and Design",[14)] $\overline{H}$ the mean wave height, $H_{1/3}$ the height of the significant wave, $H_{1/10}$ the height of the highest ten percent waves, $H_{\max}$ the maximum wave height, N the number of the analyzed waves, $\overline{T}$ the mean wave period associated with

Table 3.1 Wind-generated waves at Hakata Bay

Run No.	F	F_e	$\overline{H}$	$H_{1/3}$	$H_{1/10}$	H_{max}	N	$\overline{T}$	T_c	$T_{1/3}$	$T_{1/10}$	ϵ	$L_{1/3}$
	km	km	m	m	m	m		sec	sec	sec	sec		m
3 — 1	6.8	4.5	0.09	0.12	0.16	0.20	200	2.5	1.4	2.6	2.8	0.83	11
3 — 2	5.1	4.9	0.17	0.22	0.28	0.34	206	2.4	1.3	2.7	2.3	0.84	11
3 — 3	5.1	4.9	0.15	0.23	0.28	0.34	216	2.3	1.3	2.1	2.0	0.82	6.9
3 — 4	5.1	5.0	0.21	0.30	0.36	0.41	169	2.7	1.9	2.3	2.1	0.71	8.3
3 — 5	5.2	5.0	—	—	—	—	—	—	—	—	—	—	—
3 — 6	5.2	5.0	0.23	0.32	0.41	0.59	196	2.3	1.6	2.4	2.8	0.72	9.0
3 — 7	5.0	4.7	0.30	0.41	0.52	0.77	191	2.6	1.7	2.5	2.6	0.76	9.7
3 — 8	5.0	4.7	0.34	0.46	0.54	0.68	168	3.0	1.8	2.7	2.3	0.80	11

*) Even if we consider the fact that the wind directions at F. M. O. are measured in 16-direction and those at the tower are measured in the angle θ^0, the final conclusion will be not so different.

Table 3.2 Wind-generated waves at Hakata Bay

Run No.	F	F_e	$\overline{H}$	$H_{1/3}$	$H_{1/10}$	H_{max}	N	$\overline{T}$	$\overline{T}_c$	$T_{1/3}$	$T_{1/10}$	ϵ	$L_{1/3}$
	km	km	m	m	m	m		sec	sec	sec	sec		m
4 — 1	5.1	4.8	0.27	0.38	0.46	0.71	270	2.3	1.9	2.4	2.3	0.56	9.0
4 — 2	5.1	4.8	0.35	0.51	0.64	0.86	249	2.5	2.1	2.7	2.6	0.54	11
4 — 3	5.1	4.9	0.29	0.42	0.53	0.74	119	2.5	1.9	2.5	2.5	0.65	9.7
4 — 4	5.1	4.7	0.29	0.42	0.52	0.71	271	2.3	1.6	2.4	2.5	0.56	9.0
4 — 5	5.2	4.9	0.25	0.38	0.45	0.56	153	2.5	1.8	2.4	2.2	0.69	9.0
4 — 6	5.2	5.0	0.30	0.46	0.59	0.83	266	2.3	2.0	2.4	2.4	0.49	9.0
4 — 7	5.2	5.0	0.33	0.49	0.62	0.80	258	2.4	2.1	2.6	2.5	0.48	11
4 — 8	5.0	4.7	—	—	—	—	—	—	—	—	—	—	—
4 — 9	5.1	4.7	0.28	0.44	0.56	0.86	238	2.3	2.0	2.5	2.4	0.49	9.0
4 —10	4.9	5.7	0.48	0.75	0.95	1.25	244	2.6	2.2	2.7	2.7	0.53	11
4 —11	5.0	4.7	—	—	—	—	—	—	—	—	—	—	—
5 — 1	17.0	7.4	0.36	0.53	0.65	0.81	—	—	—	—	—	—	—
5 — 2	9.0	7.1	0.36	0.53	0.65	0.81	369	2.6	1.8	2.9	2.9	0.72	13
5 — 3	16.7	7.6	0.35	0.53	0.64	0.88	187	2.7	1.5	2.9	2.9	0.83	13
5 — 4	8.1	7.5	0.37	0.56	0.69	0.94	125	2.6	1.5	2.9	3.1	0.82	13
5 — 5	7.7	7.3	0.38	0.58	0.70	0.97	172	2.7	1.5	2.9	2.8	0.83	13

Table 3.3 Wind-generated waves at Hakata Bay

Run No.	F	F_e	$\overline{H}$	$H_{1/3}$	$H_{1/10}$	H_{max}	N	$\overline{T}$	$\overline{T}_c$	$T_{1/3}$	$T_{1/10}$	ϵ	$L_{1/3}$
	km	km	m	m	m	m		sec	sec	sec	sec		
6 — 1	4.1	6.4	0.39	0.62	0.80	1.08	115	2.8	2.3	3.0	2.9	0.57	14
6 — 2	16.0	7.1	0.42	0.69	0.86	1.11	159	2.7	2.2	3.1	3.0	0.58	15
6 — 3	4.3	6.2	0.58	0.89	1.04	1.25	160	3.0	2.4	3.3	3.2	0.60	17
6 — 4	4.1	6.4	0.53	0.85	1.10	1.34	199	3.1	2.3	3.4	3.5	0.67	18
6 — 5	3.9	6.4	0.57	0.89	1.13	1.35	181	3.3	2.6	3.6	3.7	0.62	20
6 — 6	3.9	6.4	0.53	0.78	0.94	1.22	187	3.3	2.7	3.5	3.4	0.58	19
6 — 7	8.1	7.5	—	—	—	—	—	—	—	—	—	—	—
6 — 8	9.0	7.1	—	—	—	—	—	—	—	—	—	—	—
6 — 9	3.8	6.4	—	—	—	—	—	—	—	—	—	—	—
6 —10		7.4	0.33	0.52	0.64	0.84	153	2.5	2.2	2.6	2.6	0.47	11
6 —11	4.1	6.4	0.39	0.59	0.73	1.00	139	2.8	2.2	2.8	2.8	0.62	12
6 —12	8.1	7.4	0.41	0.61	0.75	0.88	155	2.9	2.2	3.0	2.9	0.65	14
6 —13	3.8	6.4	—	—	—	—	—	—	—	—	—	—	—
6 —14	14.7	7.5	—	—	—	—	—	—	—	—	—	—	—
6 —15	8.1	7.5	—	—	—	—	—	—	—	—	—	—	—
6 —16		7.6	0.49	0.79	0.99	1.23	156	2.7	2.4	2.9	2.8	0.46	13
6 —17		7.4	0.47	0.75	0.99	1.68	104	3.0	2.4	3.1	2.8	0.60	15
6 —18	8.1	7.4	0.40	0.61	0.77	1.28	160	3.2	2.3	3.3	3.2	0.70	17
6 —19		7.4	0.34	0.54	0.69	1.32	212	2.8	2.3	2.9	2.8	0.57	13

the average time interval between successive zero up-cross of the waves, $\overline{T}_c$ the mean wave period associated with the average time interval between successive maxima of the waves, $T_{1/3}$ the period of significant wave, $T_{1/10}$ the period of the highest ten percent waves, and ϵ the spectral width[15] defined by

$$\epsilon^2=1-\left(\frac{\overline{T}_c}{\overline{T}}\right)^2. \tag{9}$$

$L_{1/3}$ is the wave length of the significant wave, which is defined by

Table 3.4 Wind-generated waves at Hakata Bay

Run No.	k	F_e	$\overline{H}$	$H_{1/3}$	$H_{1/10}$	H_{mxx}	N	$\overline{T}$	$\overline{T}_b$	$T_{1/3}$	$T_{1/10}$	ϵ	$L_{1/3}$
	km	km	m	m	m	m		sec	sec	sec	sec		m
6 —20	5.0	4.7	—	—	—	—	—	—	—	—	—	—	—
6 —21	5.1	5.0	0.31	0.46	0.58	0.93	236	2.5	1.7	2.5	2.4	0.73	9.7
6 —22		7.4	—	—	—	—	—	—	—	—	—	—	—
6 —23	14.8	7.5	0.51	0.80	1.00	1.26	192	3.1	1.9	3.3	3.2	0.79	17
6 —24	16.0	7.1	0.47	0.71	0.88	1.04	197	2.5	1.8	3.0	3.0	0.69	14
6 —25	16.5	7.6	0.60	0.91	1.11	1.30	192	3.2	2.2	3.5	3.7	0.73	19
6 —26	6.3	6.8	0.46	0.65	0.79	0.99	126	3.0	1.9	3.3	3.4	0.77	17
6 —27		4.0	0.30	0.45	0.53	0.79	195	2.4	1.5	2.7	2.6	0.78	11
6 —28	14.7	7.5	0.50	0.79	1.00	1.51	210	3.0	2.0	3.3	3.4	0.75	17
6 —29	15.3	7.5	0.59	0.94	1.22	1.86	173	3.3	2.2	3.0	3.5	0.75	14
6 —30		7.4	0.43	0.66	0.85	1.06	210	2.8	1.9	3.4	3.3	0.73	18
6 —31		7.6	—	—	—	—	—	—	—	—	—	—	—
6 —32	8.1	7.4	0.46	0.73	0.92	1.18	154	2.8	2.1	3.0	3.1	0.66	14
6 —33	7.5	7.1	0.48	0.76	1.02	1.36	133	3.2	2.4	3.4	3.1	0.66	18
6 —34	8.0	7.4	0.60	0.93	1.11	1.30	191	3.2	2.3	3.3	3.6	0.70	17
6 —35		7.4	0.49	0.73	0.87	1.13	167	3.2	2.4	3.4	3.3	0.66	18
6 —36	16.0	7.1	0.51	0.79	0.95	1.27	137	3.0	2.0	3.4	3.3	0.75	18
6 —37	16.0	7.1	0.57	0.87	1.11	1.56	218	3.0	2.1	3.2	3.3	0.71	16
6 —38	16.0	7.1	0.49	0.76	0.90	1.13	149	2.8	2.2	3.2	3.1	0.62	16

$$L_{1/3} = \frac{gT_{1/3}^2}{2\pi} \tanh \frac{2\pi h}{L_{1/3}}, \tag{10}$$

where h is the water depth.

In previous papers,[1),2),3)] on the basis of the data of the winds and waves observed respectively in Hakata Bay and in our wave tank of large scale, the following empirical formulas have been derived for wind-wave relationships:

$$\frac{gH_{1/3}}{U_{10}^2} = 2.15 \times 10^{-3} \left(\frac{gF_e}{U_{10}^2}\right)^{0.504}, \tag{11}$$

$$\frac{gT_{1/3}}{2\pi U_{10}} = 5.07 \times 10^{-2} \left(\frac{gF_e}{U_{10}^2}\right)^{0.330}. \tag{12}$$

It was also pointed out that these formulas were quite similar to Wilson's formulas IV.[16)] In order to confirm the above formulas, the dimensionless parameters were calculated from the measured wave data shown in Tables 3.1 through 3.4, and they were summarized in the left side columns of Tables 4.1 through 4.4. In Fig. 10 the relation between the dimensionless wave height $gH_{1/3}/U_{10}^2$ and the dimensionless fetch gF_e/U_{10}^2, and the relation between the dimensionless wave period $gT_{1/3}/2\pi U_{10}$ and the dimensionless fetch gF_e/U_{10}^2 were compared respectively with Eq. (11) and Eq. (12). It can be seen from Fig. 10 that the present results agree fairly well with the previous formulas Eq. (11) and Eq. (12), except for two data which are surrounded by a dotted line. Particularly, the observed relation between $gT_{1/3}/2\pi U_{10}$ and gF_e/U_{10}^2 is in satisfactory agreement with Eq. (12). Although some scatters of the data are shown in the relation between $gH_{1/3}/U_{10}^2$ and gF_e/U_{10}^2, the line of Eq. (11) passes through the

Table 4.1 Dimensionless wind-wave parameters, drag coefficicient and related parameters.

Run No.	$\frac{gF_e}{U_{10}^2}$	$\frac{gH_{1/3}}{U_{10}^2}$	$\frac{gT_{3/1}}{2\pi U_{10}}$	$\frac{H_{1/3}}{L_{1/3}}$	$\frac{C_{1/3}}{u_*}$	γ_{10}^2	$\frac{u_*\overline{H}}{\nu}$	$\frac{u_* z_0}{\nu}$	ν
	$\times 10^3$	$\times 10^{-1}$		$\times 10^{-2}$		$\times 10^{-3}$	$\times 10^4$		
3 — 1	2.4	0.64	0.94	1.1	21	1.9	0.12	12	0.149
3 — 2	1.6	0.71	0.77	1.9	18	1.9	0.27	18	0.149
3 — 3	1.3	0.59	0.53	3.3	12	1.9	0.27	18	0.149
3 — 4	0.90	0.54	0.49	3.6	11	1.8	0.45	18	0.149
3 — 5	0.87	—	—	—	—	2.0	—	32	0.149
3 — 6	0.81	0.52	0.48	3.6	12	1.6	0.48	10	0.149
3 — 7	0.56	0.49	0.43	4.2	10	1.7	0.77	17	0.149
3 — 8	0.52	0.51	0.45	4.1	9.1	2.4	1.1	80	0.149

Table 4.2 Dimensionless wind-wave parameters, drag coefficient and related parameters.

Run No	$\frac{gF_e}{U_{10}^2}$	$\frac{gH_{1/3}}{U_{10}^2}$	$\frac{gT_{1/3}}{2\pi U_{10}}$	$\frac{H_{1/3}}{L_{1/3}}$	$\frac{C_{1/3}}{u_*}$	γ_{10}^2	$\frac{u_*\overline{H}}{\nu}$	$\frac{u_* z_0}{\nu}$	ν
	$\times 10^3$	$\times 10^{-1}$		$\times 10^{-2}$		$\times 10^{-3}$	$\times 10^4$		
4 — 1	0.46	0.37	0.37	4.2	13	0.74	0.51	7.9×10^{-2}	0.148
4 — 2	0.40	0.42	0.39	4.5	15	0.64	0.67	2.5×10^{-2}	0.146
4 — 3	0.44	0.38	0.38	4.3	18	0.45	0.44	9.3×10^{-4}	0.144
4 — 4	0.44	0.40	0.37	4.7	15	0.60	0.50	1.4×10^{-2}	0.144
4 — 5	0.61	0.47	0.42	4.2	22	0.37	0.30	1.1×10^{-4}	0.144
4 — 6	0.31	0.34	0.33	5.1	11	0.95	0.73	5.4×10^{-1}	0.144
4 — 7	0.53	0.52	0.42	4.7	15	0.85	0.65	2.2×10^{-1}	0.143
4 — 8	0.41	—	—	—	—	0.66	—	3.0×10^{-2}	0.143
4 — 9	0.39	0.36	0.36	4.5	13	0.76	0.58	1.0×10^{-1}	0.144
4 —10	0.66	0.87	0.46	6.6	8.8	2.7	1.6	1.6×10^{2}	0.144
4 —11	0.43	—	—	—	—	0.64	—	2.5×10^{-2}	0.144
								$\times 10^2$	
5 — 1	1.3	0.90	0.60	4.1	9.4	4.0	1.2	6.2	0.140
5 — 2	0.76	0.56	0.47	4.1	6.3	5.4	1.8	22	0.140
5 — 3	1.1	0.74	0.54	4.1	7.8	4.8	1.5	13	0.140
5 — 4	0.93	0.69	0.51	4.3	7.9	4.0	1.5	7.3	0.141
5 — 5	1.3	1.1	0.62	4.5	10	3.7	1.2	4.1	0.141

midle of the scattered data.

Two data surrounded by a dotted line (Run 3-1, Run 3-2) deviate remarkably from the formulas. Those data were obtained in an initial stage of the wind waves where the wind speed was still low and its duration was relatively short. Therefore, the wind waves generated in the bay was still small and was affected by the small swell came from the outside of the bay. The co-existence of the swell and wind wave was substanciate previously by the spectral analysis of the wave record. Those situations might be the cause for the deviation of the data.

4.4. Wind shear stress and water surface roughness

There have been many measurements[4),17),18),19),20)] of the drag coefficient γ_{10}^2 of the sea surface, which is defined by

$$\tau_0 = \rho \gamma_{10}^2 U_{10}^2. \tag{13}$$

Table 4.3 Dimensionless wind-wave parameters, drag coefficient and related parameters.

Run No.	$\frac{gF_e}{U_{10}^2}$	$\frac{gH_{1/3}}{U_{10}^2}$	$\frac{gT_{1/3}}{2\pi U_{10}}$	$\frac{H_{1/3}}{L_{1/3}}$	$\frac{c_{1/3}}{u_*}$	$\gamma^2{}_{10}$	$\frac{u_*\overline{H}}{\nu}$	$\frac{u_* z_0}{\nu}$	ν
	$\times 10^3$	$\times 10^{-1}$		$\times 10^{-2}$		$\times 10^{-3}$	$\times 10^4$	$\times 10^2$	
6 — 1	0.55	0.53	0.44	4.5	5.7	5.9	2.3	31	0.142
6 — 2	0.39	0.38	0.36	4.7	4.7	7.1	3.1	39	0.140
6 — 3	0.39	0.56	0.41	5.3	5.8	5.0	3.7	22	0.139
6 — 4	0.47	0.63	0.46	4.8	7.4	3.7	2.7	7.2	0.138
6 — 5	0.41	0.57	0.45	4.5	7.0	4.0	3.3	9.7	0.137
6 — 6	0.42	0.51	0.44	4.2	5.7	5.7	3.6	34	0.136
6 — 7	0.52	—	—	—	—	5.0	—	22	0.136
6 — 8	0.62	—	—	—	—	5.2	—	22	0.136
6 — 9	0.96	—	—	—	—	4.4	—	10	0.133
6 —10	0.79	0.55	0.42	4.9	6.0	4.9	1.6	16	0.136
6 —11	0.57	0.52	0.42	4.8	6.7	3.9	1.9	8.1	0.136
6 —12	0.50	0.41	0.39	4.4	7.4	3.6	1.9	2.2	0.137
6 —13	0.52	—	—	—	—	3.5	—	5.7	0.138
6 —14	0.80	—	—	—	—	5.8	—	28	0.139
6 —15	0.57	—	—	—	—	4.6	—	16	0.140
6 —16	0.56	0.59	0.39	6.0	6.2	4.0	2.6	9.4	0.140
6 —17	0.73	0.74	0.48	5.0	6.9	4.9	2.4	17	0.140
6 —18	0.62	0.51	0.48	3.7	6.7	4.9	2.2	18	0.139
6 —19	0.80	0.59	0.48	4.1	6.6	5.2	1.7	19	0.138

Table 4.4 Dimensionless wind-wave parameters, drag coefficient and related parameters.

Run No.	$\frac{gF_e}{U_{10}^2}$	$\frac{gH_{1/3}}{U_{10}^2}$	$\frac{gT_{1/3}}{2\pi U_{10}}$	$\frac{H_{1/3}}{L_{1/3}}$	$\frac{c_{/13}}{u_*}$	$\gamma_{10}{}^2$	$\frac{u_*\overline{H}}{\nu}$	$\frac{u_* z_0}{\nu}$	ν
	$\times 10^3$	$\times 10^{-1}$		$\times 10^{-2}$		$\times 10^{-3}$	$\times 10^4$	$\times 10^2$	
6 —20	0.31	—	—	—	—	1.9	—	0.34	0.143
6 —21	0.52	0.48	0.40	4.7	8.0	2.5	1.1	1.2	0.141
6 —22	0.70	—	—	—	—	4.9	—	17	0.135
6 —23	0.62	0.66	0.47	4.8	7.7	3.6	2.5	6.4	0.134
6 —24	0.59	0.59	0.43	5.1	7.0	3.7	2.4	7.0	0.134
6 —25	0.49	0.59	0.44	4.9	6.3	4.8	3.8	20	0.134
6 —26	0.69	0.66	0.53	3.9	8.2	3.8	2.0	6.7	0.135
6 —27	0.64	0.73	0.54	4.0	11	2.6	0.86	1.2	0.139
6 —28	0.38	0.40	0.37	4.7	5.8	4.0	3.3	12	0.133
6 —29	0.54	0.67	0.40	6.7	6.8	3.5	3.1	5.8	0.132
6 —30	0.46	0.41	0.42	3.8	5.2	6.4	2.9	46	0.148
6 —31	0.64	—	—	—	—	7.1	—	56	0.146
6 —32	0.46	0.46	0.37	5.2	5.3	5.0	2.8	21	0.144
6s—33	0.46	0.49	0.43	4.3	5.8	5.2	3.0	24	0.144
6 —34	0.39	0.49	0.38	5.6	4.2	7.6	5.0	83	0.144
6 —35	0.43	0.42	0.41	4.2	4.4	8.2	4.0	98	0.144
6 —36	0.48	0.53	0.44	4.5	6.2	4.7	3.2	19	0.133
6 —37	0.43	0.52	0.39	5.5	6.0	4.1	3.5	12	0.133
6 —38	0.46	0.49	0.41	4.8	5.5	5.3	3.3	28	0.133

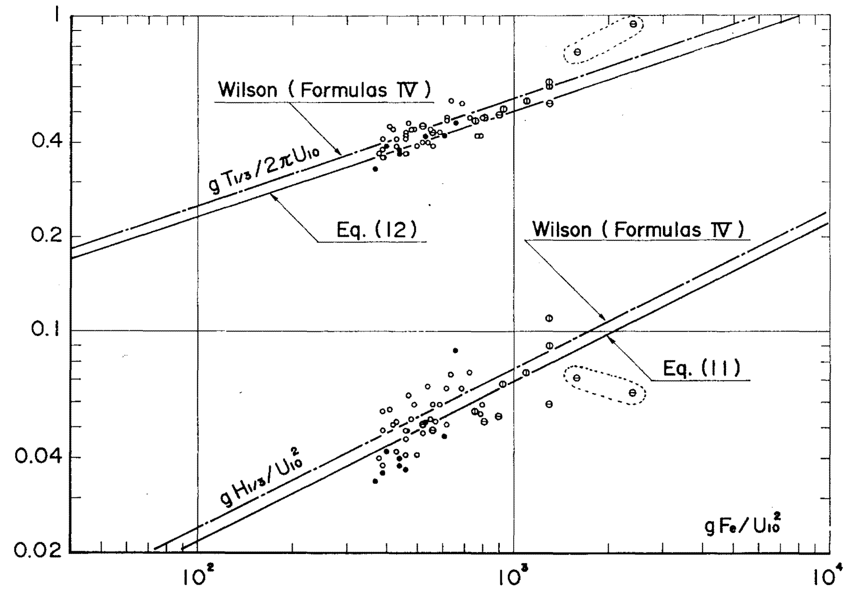

Fig. 10 Relationships of wind-wave parameters

From those various measurements it has been shown that when the wind speed is small, say, $U_{10}<3$ m/s, γ_{10}^2 is close to the value for aerodynamically smooth flow, while when $U_{10}>3$ m/s, γ_{10}^2 has a tendency to increase with increasing the wind speed U_{10}. However, the considerable scatter has been found in those measurements and the definite relationship between γ_{10}^2 and U_{10} has not been determined yet.

In our previous measurements[2)] in Hakata Bay, γ_{10}^2 was in the range of $1\times10^{-3}\sim2\times10^{-3}$ within the range of the wind velocity U_{10}: 2 m/s$\sim$9 m/s, and γ_{10}^2 was seemed, in many cases, to increase with the wind speed U_{10}, though there was one exceptional case in which γ_{10}^2 decreased with increasing U_{10}. In order to clarify those controversial characteristics of γ_{10}^2, the present wind data have been analyzed.

From Eq. (2) and Eq. (13) it follows

$$u_*^2 = \gamma_{10}^2 U_{10}^2. \tag{14}$$

Therefore, γ_{10}^2 can be determined from the measured values of u_* and U_{10}. The determined values of γ_{10}^2 are summarized in the right side columns of Tables 5.1 through 5.4 together with various parameters relating to γ_{10}^2. Fig. 11 shows the relation between γ_{10}^2 and U_{10}. As can be seen from Fig. 11 the scatter of the measured value of γ_{10}^2 is considerable, but there are shown several interesting characteristics of γ_{10}^2. That is, when $U_{10}>7$ m/s, γ_{10}^2 increases rapidly with increasing U_{10} and it attaines to a very large value except for the data of Run 4-1$\sim$9 and Run 4-11 which show very small values. When we

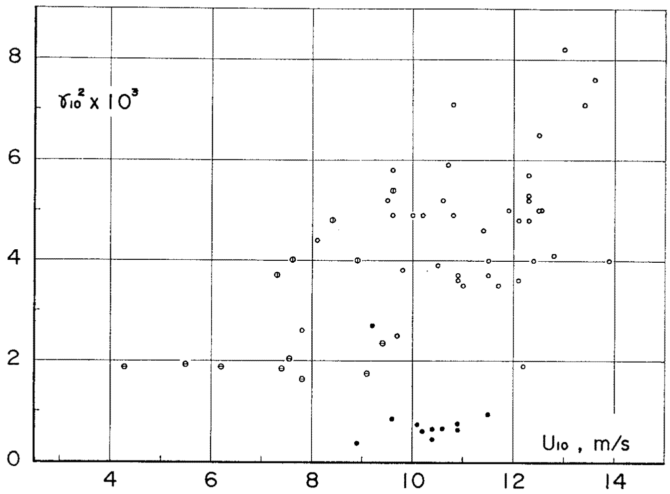

Fig. 11 The drag coefficient γ_{10}^2 of the sea surface as a function of wind speed U_{10}.

consider that the values of γ_{10}^2 measured by many investigators are atmost 3×10^{-3}, the present values scattered in the range from 2×10^{-3} to 8×10^{-3} are remarkably large. As shown previously in Figs. 7.1 through 7.5, most of the wind profiles have been very close to the logarithmic profiles, and thus the present values of γ_{10}^2 determined from the wind profiles are considered to be reliable. Recently, Toba & Kunishi (1970)[21] obtained a more universal expression for γ_{10}^2 by introducing the roughness Reynolds number $u_* \overline{H}/\nu$ where u_* is the friction velocity of the air, $\overline{H}$ the mean wave height, and ν the kinematic viscosity of the air. By using the data of the wind and waves measured in their wind flumes, they determined the relationship between γ_{10}^2 and $u_*\overline{H}/\nu$ in which the scatters of the data were remarkably reduced. Moreover, it is interesting to find that the values of γ_{10}^2 measured in their high speed wind flume have increased rapidly with increasing $u_*\overline{H}/\nu$ and it attaines to such a large value as $\gamma_{10}^2 \doteqdot 5.5 \times 10^{-3}$ at $u_*\overline{H}/\nu \doteqdot 5 \times 10^4$. Our present data have been compared, in Fig. 12, with the results obtained by Toba & Kunishi (1970). In Fig. 12 the data of Toba & Kunishi (1970) are shown by their average line (solid line) and the range of their scatters (broken line). It can be seen from Fig. 12 that the results obtained in the present investigation are quite similar to those obtained by Toba & Kunishi except for a group of data (Run 4-1~9, Run 4-11) surrounded by dotted line. The reason why the data of Run 4-1 ~9 and Run 4-11 have been so different from the other data is not clear at this time, because the wind profiles corresponding to those data have been very close to the logarithmic profiles as shown previously in Fig. 7.2. In any events, the result shown in Fig. 12 must be one of the most interesting results of the present study. Fig. 13 shows the relation between the

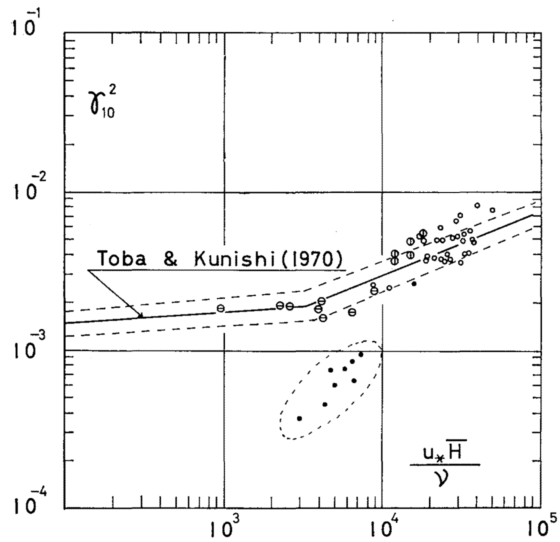

Fig. 12 The drag coefficient r_{10}^2 of the sea surface related to the roughness Reynolds number $u_*\overline{H}/\nu$.

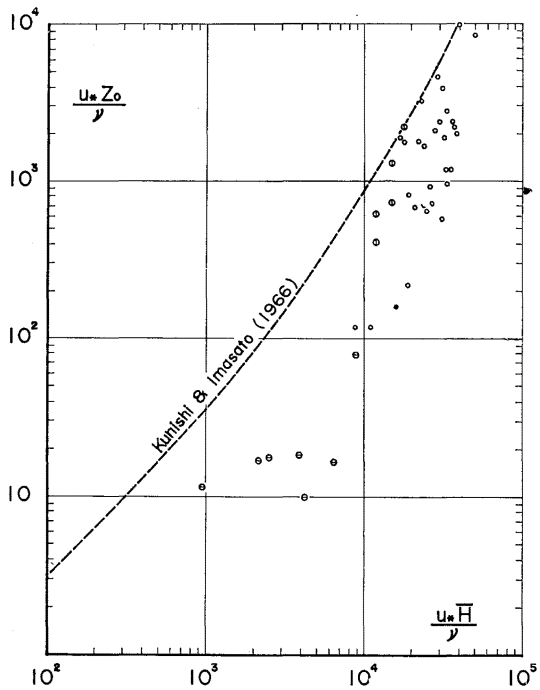

Fig. 13 The dimensionless roughness parameter u_*z_0/ν of the sea surface related to the roughness Reynolds number $u_*\overline{H}/\nu$.

dimensionless roughness parameter $u_* z_0/\nu$ and the roughness Reynolds number $u_* \overline{H}/\nu$, in which measured data are compared with the results obtained by Kunishi & Imasato (1966)[22] in their high speed wind flum. Here again we can see a similarities in the results obtained respectively in a wind flume and in the bay, though their absolute values are different, and some of the present data (Run 4-1~9, Run 4-11) are far below the figure ; $u_* z_0/\nu < 1$. The parameters $u_* \overline{H}/\nu \cdot \exp(-kc/u_*)$ derived by Kitaigorodskii (1968)[20] and $u_* \overline{H}/\nu \cdot (H/L)^2$ derived by Iwata (1969)[23] have been related to γ_0^2 or $u_* z_0/\nu$, but the scatter of the data has been not so reduced.

5. Concluding Remarks

The measured result shown in Fig. 12 is parhaps one of the most interesting findings of the present investigation, because it shows a close similarity between the characteristics of the drag coefficient measured in the laboratory flume and those measured in the sea. Moreover, it is very interesting to have measured such large value of γ_{10}^2 as 8×10^{-3} in the sea, because the maximum values hitherto observed in the sea has been approximately 3×10^{-3}. However, the reasons why the past data have not shown such large values as observed in the present measurement, are not clear now. Further, it should be noted that the scatter of the present data of γ_{10}^2 are fairly large. This fact suggests that more parameters are needed for clarfying the problems of wind shear stress excerted on the water surface. For this purpose the data are being subjected to more detailed analysis.

Acknowledgements

The authors express their gratitude to Dr. S. Mizuno for his valuable comments on the first draft of this paper, to Mr. K. Eto for the constant assistance in carrying out the observations, and to Miss N. Negoro for her typing of the manuscript.

The observations described here has been greatly supported by the 4th Regional Bureau of Port and Harbour Construction, Ministry of Transportation. The authors are much indebted to the director and the staff of the Bureau.

References

1) Mitsuyasu, H., On the Growth of the Spectrum of Wind-Generated Waves (1), Rep. Res. Inst. Appl. Mech., Vol. XVII, No. 55, 1968, 459-482.
2) Mitsuyasu, H. and Nakayama, R., On the Observations of the Wind and Waves in Hakata Bay, (in Japanese), Bull. Res. Inst. Appl. Mech., No. 33, 1969, 33-66.
3) Mitsuyasu, H., On the Growth of the Spectrum of Wind-Generated Waves — A Form of Wave Spectrum at Short Fetches —, (in Japanese), Bull. Res. Inst. Appl. Mech., No. 34, 1970, 65-76.
4) Roll, H. U., *Physics of the Marine Atmosphere*. Academic Press, 1965, p. 426.
5) Monin, A. S. and Obukov, A. M., The Basic Regularity in Turbulent Mixing in

the Surface Layer, Trudy Geophys. Inst. Akad. Nauk, USSR, 24, 1954, 163-187.
6) Taylor, R. J., Similarity Theory in the Relation between Fluxes and Gradients in the Lower Atmosphere, Quart. J. Roy. Met. Soc., 86, 1960, 67-78.
7) Panofsky, H. and R. A. McCormic, The Spectrum of Vertical Velocity near the Surface, Quart. J. Roy. Met. Soc., 86, 1960, 495-503.
8) Takeda, A., Wind Profiles over Sea Waves, J. Oceanogr. Soc. Japan, 19, 1963, 136-142.
9) Nan'nichi, T., Fujiki, A. and Akamatsu, H., Micro-Meteorological Observations over the Sea (I). J. Oceanogr. Soc. Japan, Vol. 24, No. 6, 1968, 281-294.
10) Stewart, R. W., The Wave Drag of Wind over Water, J. Fluid Mech., 10, 1961, 189-194.
11) Hunt, M., Wind Effect on Water Surface, La Houille Blanche, 4, 1956, 575-607.
12) Panofsky, H. A. and Townsend, A. A., Change of Terrian Roughness and the Wind Profiles, Quart. J. Roy. Met. Soc., 90, 1964, 147-155.
13) Taylor, P. A., Wind and Shear Stress Profiles above a Change in Surface Roughness, Quart. J. Roy. Met. Soc., 95, 1969, 77-91.
14) Beach Erosion Board, Shore Protection Planning and Design, Tech. Rep. No. 4, Dept. Army, Corps of Engineers, U. S. A., 1961, p. 401.
15) Cartwright, D. E. and Longuet-Higgins, M. S., The Statistical Distribution of the Maxima of a Random Function, Proc. Roy. Soc. A. 273 (1209), 1956, 212-232.
16) Wilson, B. W., Numerical Prediction of Ocean Waves in the North Atlantic for December 1959, Deutsche Hydrogr. Zeit., 18 (3), 1965, 114-130.
17) Toba, Y., *Air-Sea Boundary Process. Physical Oceanography I, Part II, A Fundamental Course of Ocean Science, Vol. 1,* Tōkai University Press (in Japanese), 145-263.
18) Deacon, E. L. and Webb, E. K., *Interchange of Propetrties between Sea and Air, CH. 3, Small-Scale Interaction, in The Sea,* Interscience, 1962, 43-87.
19) Phillips, O. M., *The Dynamics of the Upper Ocean,* Cambridge Univ. Press., 1966, p. 261.
20) Kitaigorodskii, S. A., On the Calculation of the Aerodynamic Roughness of the Sea Surface. Izv. Atmos. Ocean. Phys. Ser. 4, 1968, 870-878.
21) Toba, Y. and Kunishi, H., Breaking of Wind Waves and the Sea Surface Wind Stress, J. Oceanogr. Soc. Japan, 26, 1970, 71-80.
22) Kunishi, H. and Imasato, T., On the Growth of the Wind-Generated Waves in High-Speed Wind Flume, (in Japanese), Disasters Prevention Res. Inst. Kyoto Univ., No. 9, 1966, 667-676.
23) Iwata, N., Aerodynamic Roughness of the Sea Surface, Bull de la Soc. Franco-japonaise d'océanographic, Tome 7, No. 4, 1969, 21-29.

(Received April 3, 1971)

Appendix

Weather maps (Japan Standard Time 0300) during the observations of the wind and waves at Hakata Bay

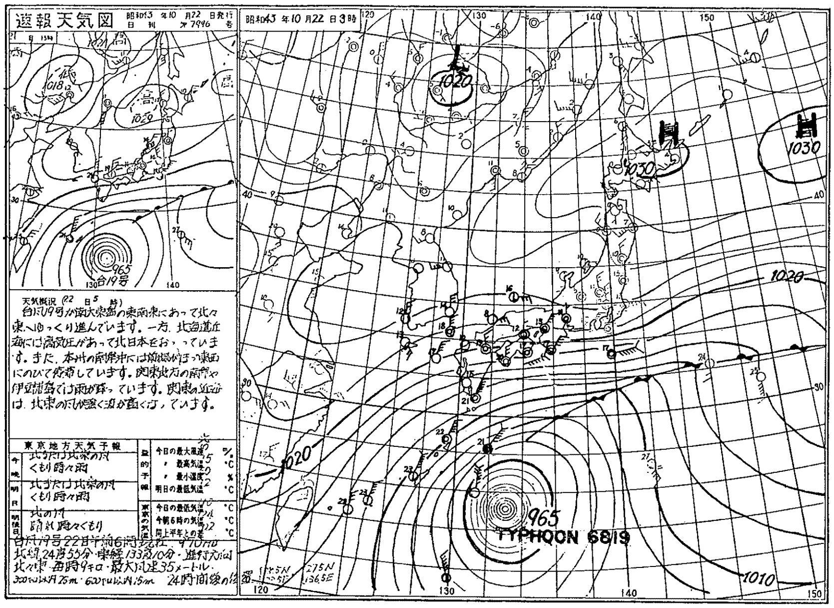

Fig. A1 Weather map for the observations Run 3-1～8 (10/22/'68).

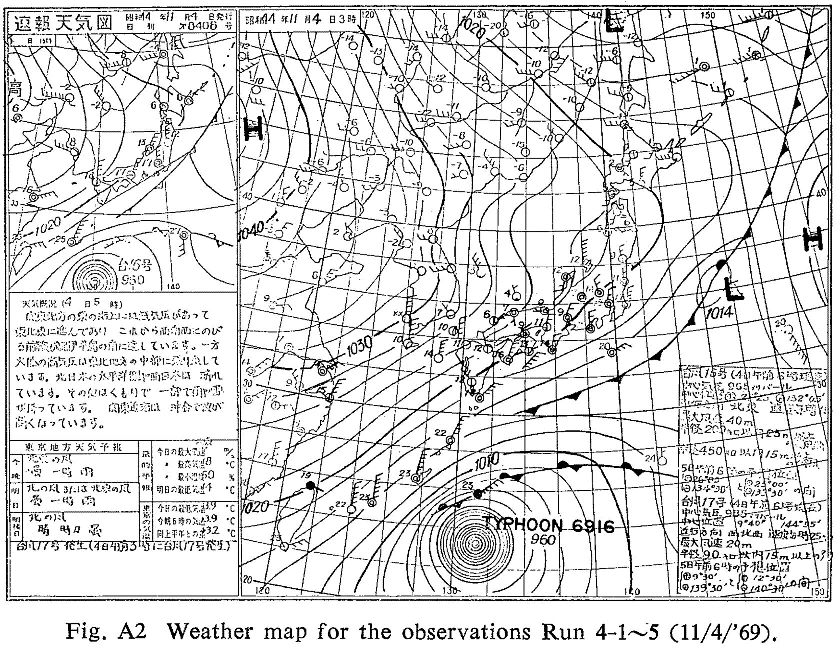

Fig. A2 Weather map for the observations Run 4-1～5 (11/4/'69).

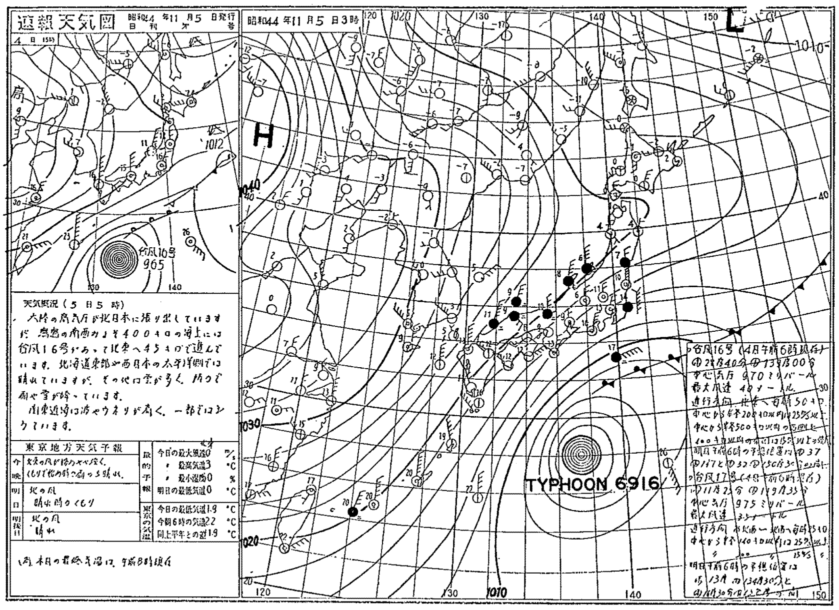

Fig. A3 Weather map for the observations Run 4-6∼11 (11/5/'69).

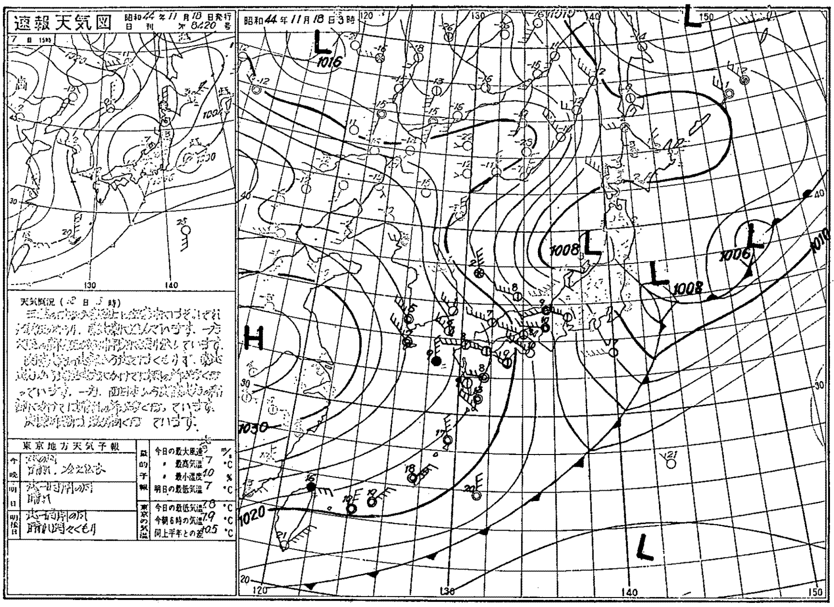

Fig. A4 Weather map for the observations Run 5-1∼5 (11/18/'69).

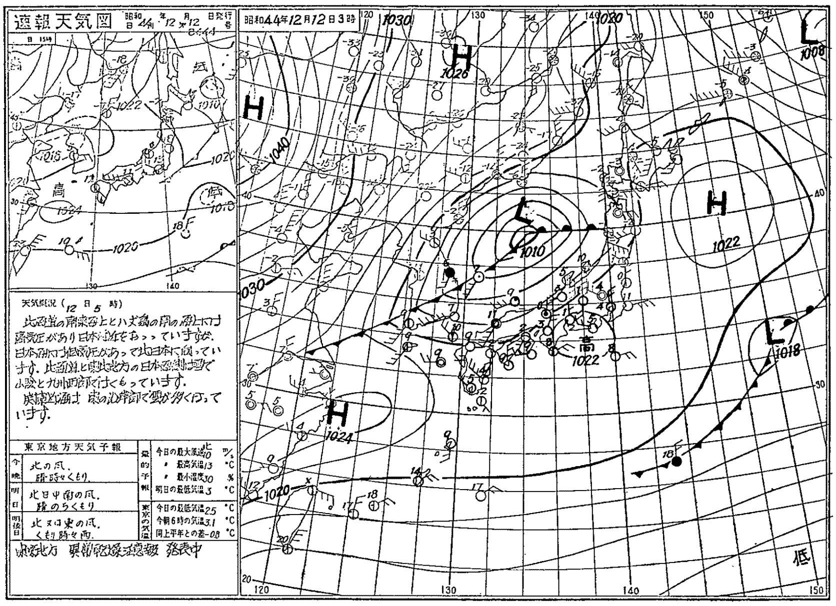

Fig. A5 Weather map for the observations Run 6-1～3 (12/12/'69).

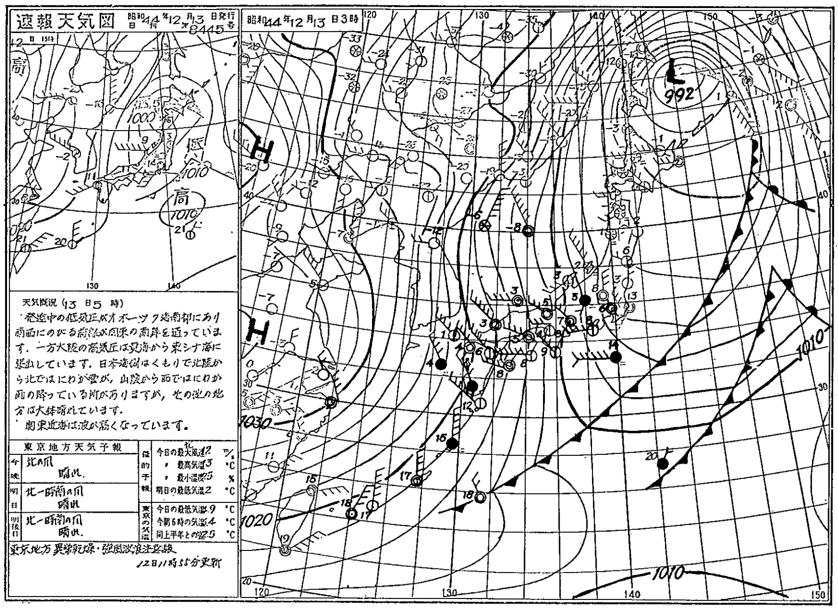

Fig. A6 Weather map for the observations Run 6-4～10 (12/13/'69).

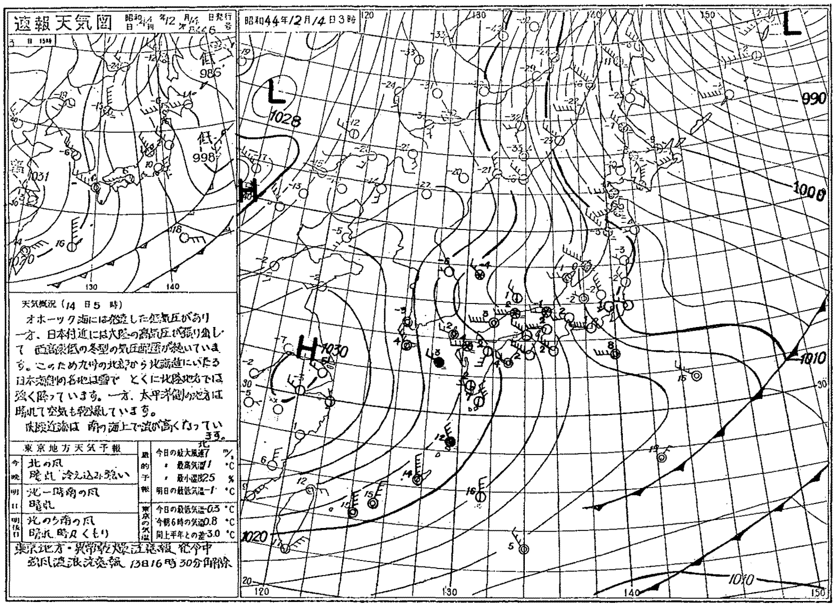

Fig. A7 Weather map for the observations Run 6-11～12 (12/14/'69).

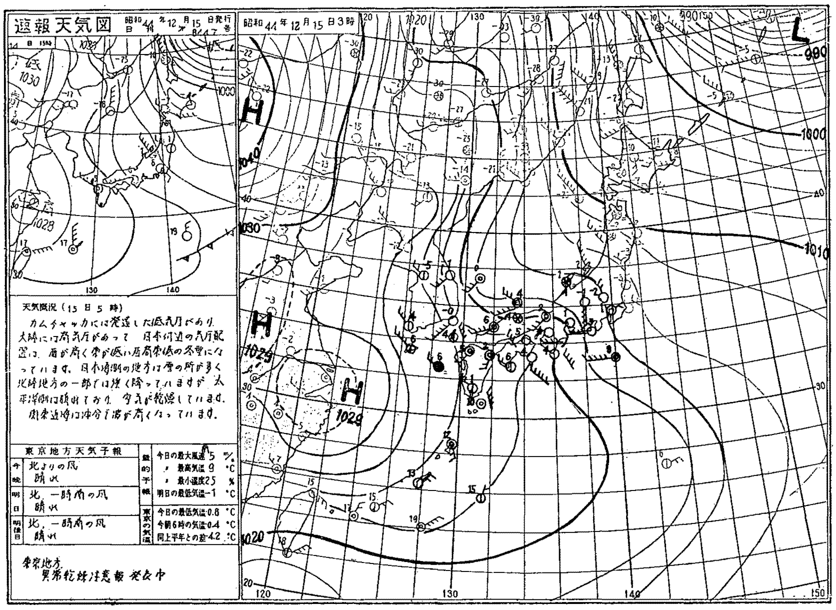

Fig. A8 Weather map for the observations Run 6-13～18 (12/15/'69).

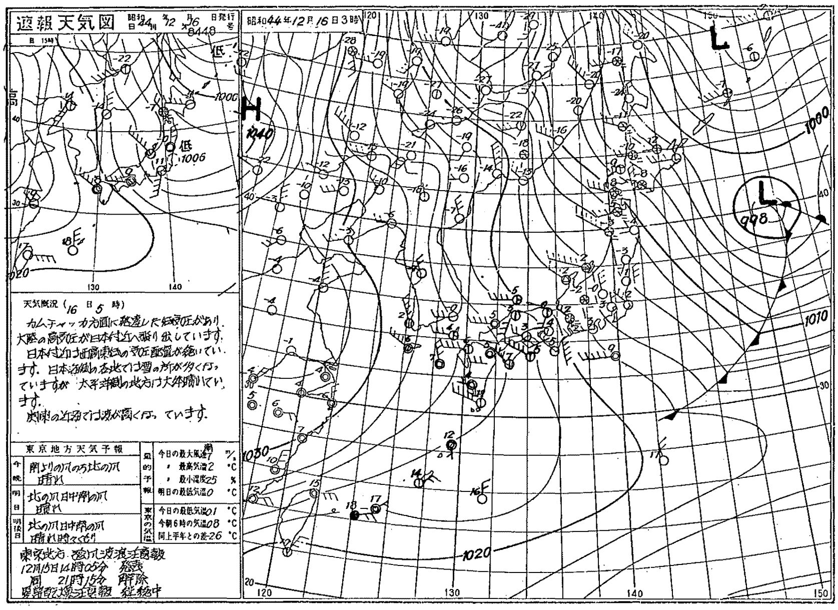

Fig. A9 Weather map for the observations Run 6-19 (12/16/'69).

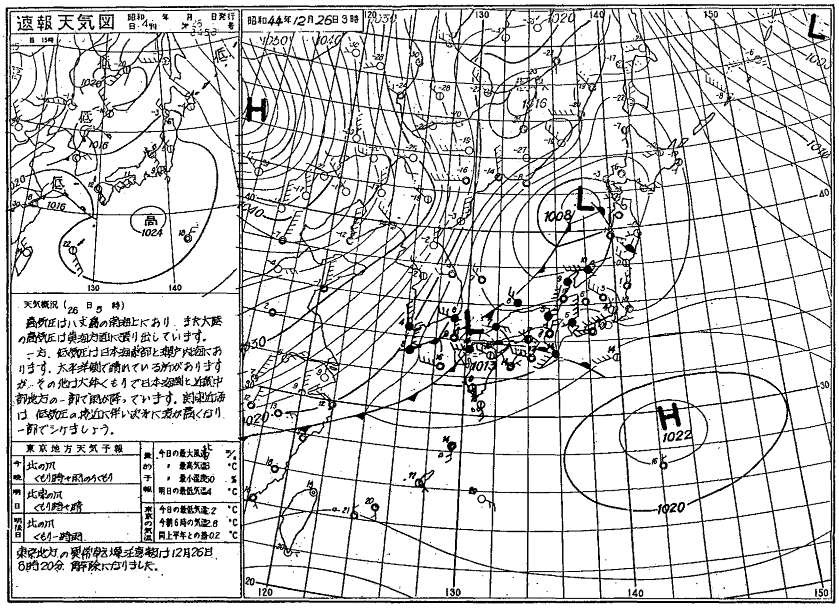

Fig. A10 Weather map for the observations Run 6-20~21 (12/26/'69).

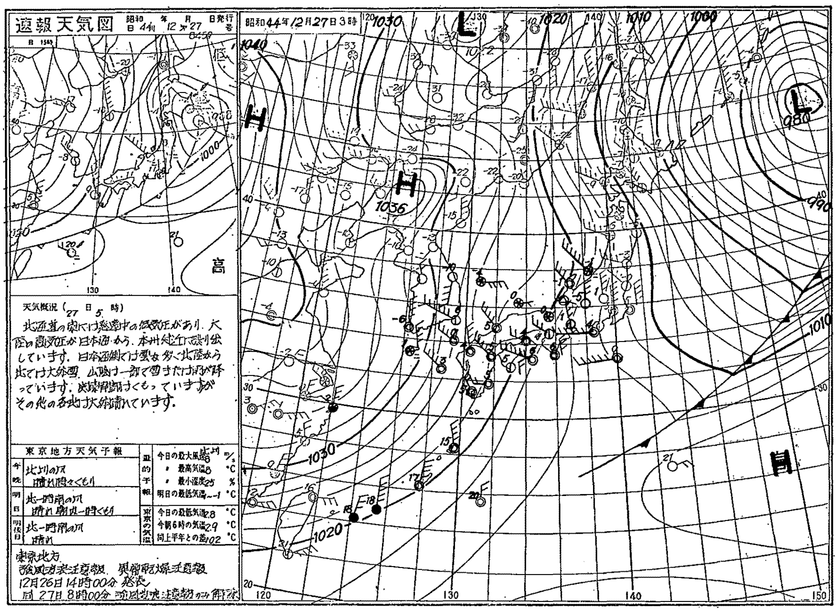

Fig. A11 Weather map for the observations Run 6-22~23 (12/27/'69).

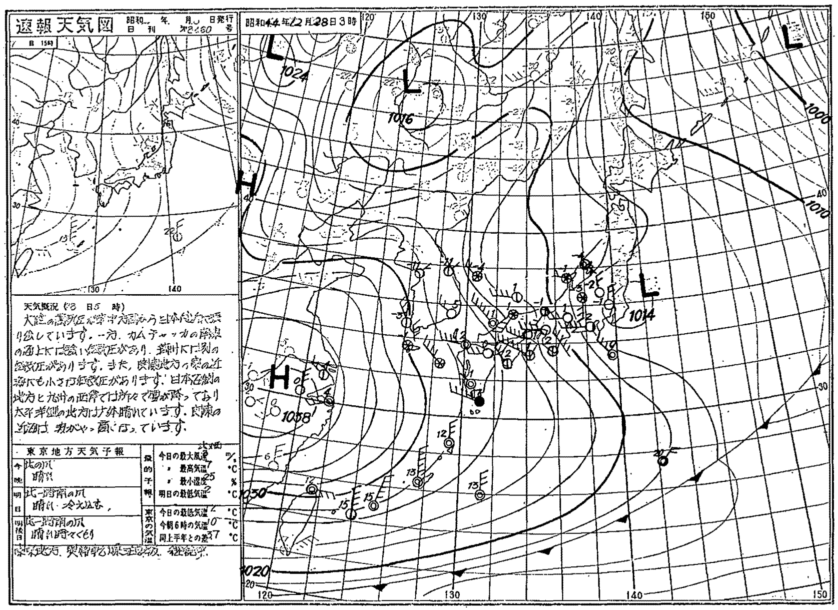

Fig. A12 Weather map for the observations Run 6-24~26 (12/28/'69).

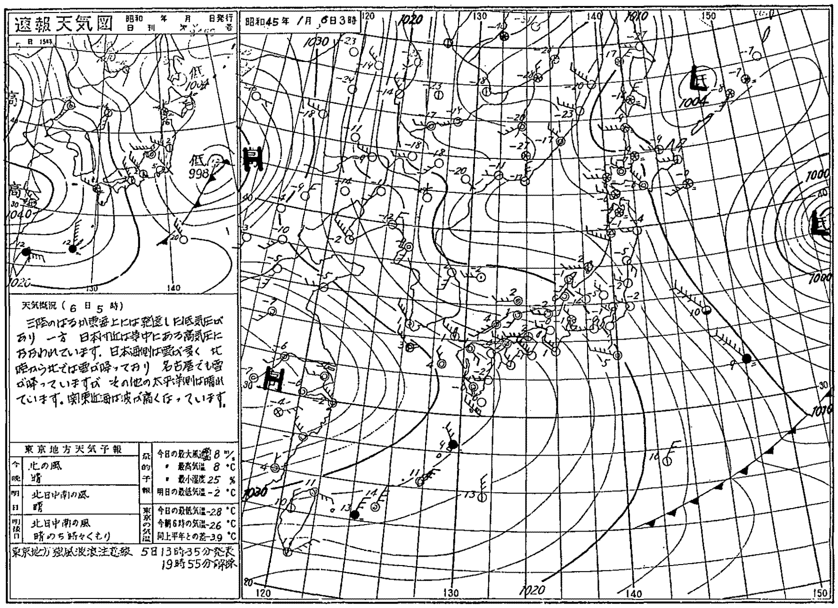

Fig. A13 Weather map for the observations Run 6-27 (1/6/'70).

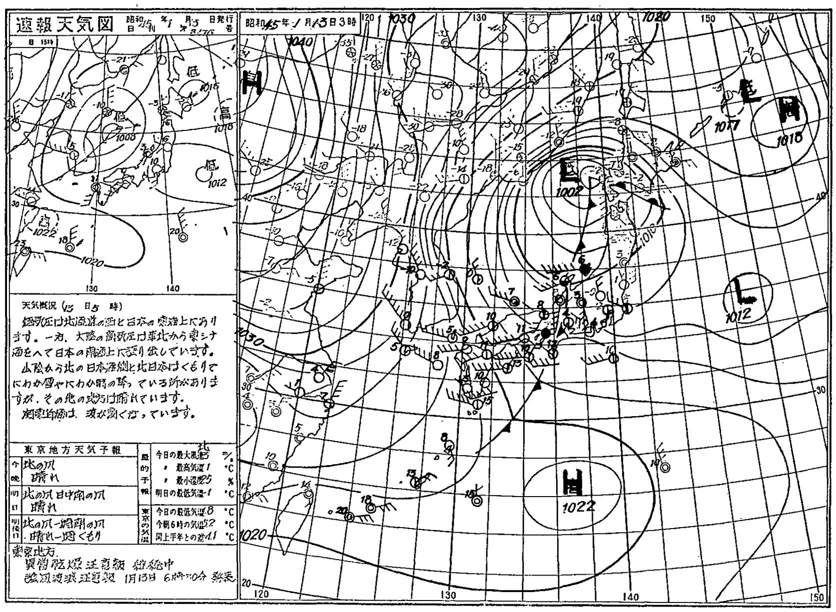

Fig. A14 Weather map for the observations Run 6-28~31 (1/13/'70).

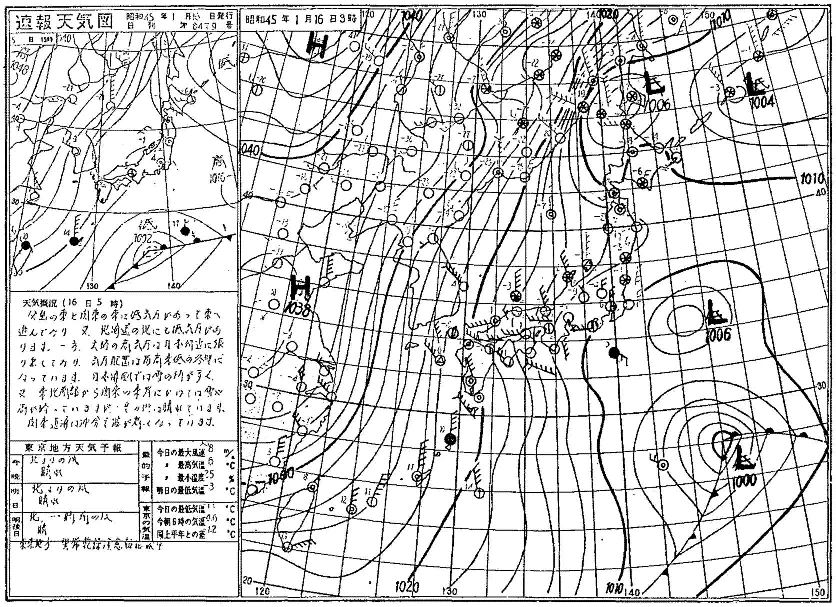

Fig. A15 Weather map for the observations Run 6-32~34 (1/16/'70).

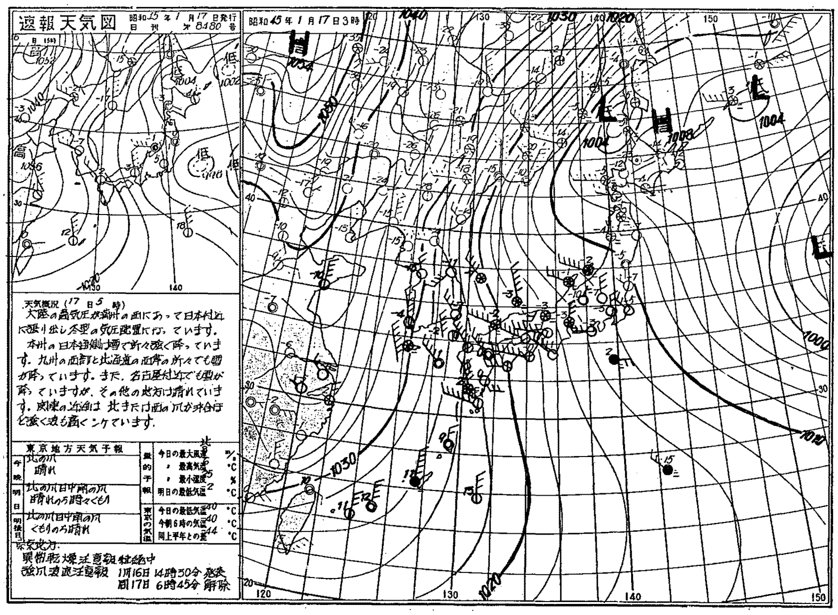

Fig. A16 Weather map for the observations Run 6-35~38 (1/17/'70).